



**HAL**  
open science

# PPAR $\gamma$ activation modulates the balance of peritoneal macrophage populations to suppress ovarian tumor growth and tumor-induced immunosuppression

Mélissa Prat, Kimberley Coulson, Clément Blot, Godefroy Jacquemin, Mathilde Romano, Marie-Laure Renoud, Mohamad Alaeddine, Augustin Le Naour, Hélène Authier, Mouna Chirine Rahabi, et al.

## ► To cite this version:

Mélissa Prat, Kimberley Coulson, Clément Blot, Godefroy Jacquemin, Mathilde Romano, et al.. PPAR $\gamma$  activation modulates the balance of peritoneal macrophage populations to suppress ovarian tumor growth and tumor-induced immunosuppression. *Journal for Immunotherapy of Cancer*, 2024, 11 (8), pp.e007031. 10.1136/jitc-2023-007031 . hal-04614101

**HAL Id: hal-04614101**

**<https://ut3-toulouseinp.hal.science/hal-04614101v1>**

Submitted on 17 Jun 2024


**HAL** is a multi-disciplinary open access archive for the deposit and dissemination of scientific research documents, whether they are published or not. The documents may come from teaching and research institutions in France or abroad, or from public or private research centers.

L'archive ouverte pluridisciplinaire **HAL**, est destinée au dépôt et à la diffusion de documents scientifiques de niveau recherche, publiés ou non, émanant des établissements d'enseignement et de recherche français ou étrangers, des laboratoires publics ou privés.



Distributed under a Creative Commons Attribution - NonCommercial 4.0 International License

# PPAR $\gamma$ activation modulates the balance of peritoneal macrophage populations to suppress ovarian tumor growth and tumor-induced immunosuppression

Mélissa Prat,<sup>1</sup> Kimberley Coulson,<sup>1</sup> Clément Blot,<sup>1</sup> Godefroy Jacquemin,<sup>1</sup> Mathilde Romano,<sup>1</sup> Marie-Laure Renoud,<sup>1</sup> Mohamad AlaEddine,<sup>1</sup> Augustin Le Naour,<sup>2</sup> Hélène Authier,<sup>1</sup> Mouna Chirine Rahabi,<sup>1</sup> Khaddouj Benmoussa,<sup>1</sup> Marie Salon,<sup>1</sup> Mélissa Parny,<sup>1</sup> Jean-Pierre Delord,<sup>3</sup> Gwenaël Ferron,<sup>3</sup> Lise Lefèvre,<sup>1</sup> Bettina Couderc,<sup>2,3</sup> Agnès Coste <sup>1</sup>

**To cite:** Prat M, Coulson K, Blot C, *et al.* PPAR $\gamma$  activation modulates the balance of peritoneal macrophage populations to suppress ovarian tumor growth and tumor-induced immunosuppression. *Journal for ImmunoTherapy of Cancer* 2023;**11**:e007031. doi:10.1136/jitc-2023-007031

► Additional supplemental material is published online only. To view, please visit the journal online (<http://dx.doi.org/10.1136/jitc-2023-007031>).

MP, KC and CB contributed equally.

LL, BC and AC are joint senior authors.

Accepted 31 July 2023



© Author(s) (or their employer(s)) 2023. Re-use permitted under CC BY-NC. No commercial re-use. See rights and permissions. Published by BMJ.

For numbered affiliations see end of article.

## Correspondence to

Dr Agnès Coste;  
agnes.coste@univ-tlse3.fr

## ABSTRACT

**Background** Ovarian adenocarcinoma (OVAD) frequently metastasizes to the peritoneal cavity and manifests by the formation of ascites, which constitutes a tumor-promoting microenvironment. In the peritoneal cavity, two developmentally, phenotypically and functionally distinct macrophage subsets, immunocompetent large peritoneal macrophages (LPM) and immunosuppressive small peritoneal macrophages (SPM), coexist. Because peroxisome proliferator-activated receptor  $\gamma$  (PPAR $\gamma$ ) is a critical factor participating in macrophage differentiation and cooperates with CCAAT/enhancer binding protein  $\beta$  (C/EBP $\beta$ ), a transcription factor essential for SPM-to-LPM differentiation, PPAR $\gamma$  could be also involved in the regulation of SPM/LPM balance and could be a promising therapeutic target.

**Methods** To evaluate the 15(S)-hydroxyeicosatetraenoic acid (HETE), a PPAR $\gamma$  endogenous ligand, impact on ovarian tumor growth, we intraperitoneally injected 15(S)-HETE into a murine ovarian cancer model. This experimental model consists in the intraperitoneally injection of ID8 cells expressing luciferase into syngeneic C57BL/6 female mice. This ID8 orthotopic mouse model is a well-established experimental model of end-stage epithelial OVAD. Tumor progression was monitored using an in vivo imaging system. Peritoneal immune cells in ascites were analyzed by flow cytometry and cell sorting. To determine whether the impact of 15(S)-HETE in tumor development is mediated through the macrophages, these cells were depleted by injection of liposomal clodronate. To further dissect how 15(S)-HETE mediated its antitumor effect, we assessed the tumor burden in tumor-bearing mice in which the PPAR $\gamma$  gene was selectively disrupted in myeloid-derived cells and in mice deficient of the recombination-activating gene *Rag2*. Finally, to validate our data in humans, we isolated and treated macrophages from ascites of individuals with OVAD.

**Results** Here we show, in the murine experimental model of OVAD, that 15(S)-HETE treatment significantly suppresses the tumor growth, which is associated with the differentiation of SPM into LPM and the LPM residency in the peritoneal cavity. We demonstrate that C/EBP $\beta$  and GATA6 play a central role in SPM-to-LPM differentiation and in LPM peritoneal residence through PPAR $\gamma$  activation during OVAD. Moreover, this SPM-to-LPM switch is

## WHAT IS ALREADY KNOWN ON THIS TOPIC

- ⇒ Among cells present in the ovarian tumor ascites, immunocompetent large peritoneal macrophages (LPM) and immunosuppressive small peritoneal macrophages (SPM) play a dual role in the promotion of ovarian tumorigenesis and cancer cell chemoresistance.
- ⇒ Data suggest that the differentiation of protumor SPM towards LPM could decrease tumor progression.
- ⇒ Peroxisome proliferator-activated receptor  $\gamma$  (PPAR $\gamma$ ) participates in macrophage differentiation and cooperates with CCAAT/enhancer binding protein  $\beta$  (C/EBP $\beta$ ), critical transcription factor for SPM-to-LPM differentiation, highlighting these transcription factors in the regulation of SPM/LPM balance.

## WHAT THIS STUDY ADDS

- ⇒ PPAR $\gamma$  activation by 15(S)-HETE ligand, inhibits tumor progression in vivo on a murine model of ovarian adenocarcinoma (OVAD).
- ⇒ PPAR $\gamma$  activation promotes the differentiation of SPM towards antitumor LPM and the LPM maintenance in the peritoneum through C/EBP $\beta$  and GATA6 activation which contribute to counteracting cancer immunosuppression.
- ⇒ 15(S)-HETE treatment improves the effector/regulatory T-cell ratio in tumor ascites through a macrophage-dependent mechanism.

## HOW THIS STUDY MIGHT AFFECT RESEARCH, PRACTICE OR POLICY

- ⇒ PPAR $\gamma$  suppression of ovarian tumor growth and tumor-induced immunosuppression, highlights this nuclear receptor as a therapeutic target to restrain OVAD development and strengthen PPAR $\gamma$  agonist use in anticancer therapy.

associated with the increase of the effector/regulatory T-cell ratio. Finally, we report that 15(S)-HETE attenuates immunosuppressive properties of human ovarian tumor-associated macrophages from ascites.

**Conclusion** Altogether, these results promote PPAR $\gamma$  as a potential therapeutic target to restrain OVAD development and strengthen the use of PPAR $\gamma$  agonists in anticancer therapy.

## INTRODUCTION

Ovarian adenocarcinoma (OVAD) has the highest mortality rate among gynecological malignancies, the main reason for which is that about 60% of patients present an extensive peritoneal carcinomatosis and most of them relapse within 12–18 months after therapy.<sup>1</sup> Platinum salts and taxanes have been the primary treatments for patients with ovarian cancer for many decades. The recent introduction of poly-ADP ribose polymerase inhibitors into the treatment plan and the improvement of surgical techniques have increased the 5-year survival rate,<sup>2</sup> but it remains at less than 50%.

Similar to many cancers, a chronic inflammation at the site of the ovarian epithelium is associated with increased ovarian cancer risk.<sup>3–5</sup> As the ovarian tumor grows, in addition to the local inflammation, tumor ascites, which contains a complex mixture of soluble factors and cellular components, provides a proinflammatory and tumor-promoting microenvironment in the peritoneal cavity.<sup>6</sup> We previously highlighted the importance of the ascites in the promotion of ovarian tumorigenesis and the acquisition of cancer cell chemoresistance through a macrophage-dependent mechanism.<sup>7</sup>

Among cells in the ovarian tumor microenvironment and ascites, tumor-associated macrophages (TAMs) are the most abundant infiltrating immune cells.<sup>8</sup> Through their plasticity, macrophages can exert a critical role in the orientation of the inflammatory response and hence the tumor development. In established tumors, TAMs produce growth factors (eg, epithelial growth factor, angiogenic factors (eg, vascular endothelial growth factor (VEGF)) and proteases (eg, matrix metalloproteinases-9 (MMP-9)) that favor tumor-cell proliferation and survival, angiogenesis, and metastasis.<sup>9,10</sup> TAMs also exhibit potent anti-inflammatory and immunosuppressive functions. TAMs present tumor-associated antigens poorly<sup>11</sup> and directly prevent T-cell activation by producing immunosuppressive factors (eg, interleukin (IL)-10 and transforming growth factor (TGF)- $\beta$ ) and upregulating immune checkpoints (eg, programmed death ligand-1 (PDL-1), PDL-2 and cytotoxic T lymphocytes antigen 4 that suppress T-cell receptor signal.<sup>9,12</sup> TAMs can also suppress CD4<sup>+</sup> and CD8<sup>+</sup> T-cell effector functions indirectly by recruiting regulatory T cells (Tregs) via CCL17 (C-C motif chemokine Ligand-17) and CCL22 production.<sup>13</sup> Moreover, the antitumor immunity of proinflammatory macrophages involves their release of proinflammatory cytokines, reactive nitrogen and oxygen intermediates that can also enhance neoplastic transformation, immunosuppression and metastatic potential of several cancers including OVAD.<sup>14–17</sup>

Increasing evidence supports that TAMs complexity and heterogeneity depend not only on their activation status but also their ontogeny.<sup>18,19</sup> Although peripheral blood monocytes are long considered to be intermediates in the differentiation of tissue macrophages, several organ-resident macrophages have an embryonic origin.<sup>19</sup> Thus,

cavity macrophages are derived from primitive precursors and self-maintained locally under steady-state without a significant input from circulating monocytes.<sup>20–22</sup> In non-steady state, such as cancers, macrophage populations of different origins can coexist in a tissue. In the peritoneal cavity, two physically, functionally and developmentally distinct macrophage subsets, large peritoneal macrophages (LPM) and small peritoneal macrophages (SPM), coexist.<sup>23</sup> While LPM (F4/80<sup>high</sup>, CD11b<sup>high</sup>, MHCII<sup>low</sup>), which are immunocompetent and appear to be originated from embryonic precursors, are more abundant under steady state conditions, SPM (F4/80<sup>low</sup>, CD11b<sup>low</sup>, MHCII<sup>high</sup>), which are immunosuppressive and generated from bone-marrow myeloid precursors, become prevalent in inflammatory conditions.<sup>24</sup>

After inflammatory or infectious stimuli, the increase of SPM is accompanied by LPM disappearance, also called macrophage disappearance reaction (MDR).<sup>25</sup> This LPM disappearance is associated with the LPM migration into the omentum due to reduced expression of GATA6. GATA6 is a major transcription factor involved in the emergence of peritoneal macrophage identity.<sup>26</sup> In conditions that LPM are greatly reduced, SPM can differentiate into LPM, hence participating in the maintenance of LPM in the peritoneal cavity.<sup>27</sup> In a murine model of ovarian cancer, SPM are enriched for proinflammatory and proangiogenic factors that promote ovarian cancer cell proliferation and mobilization in response to IL-17 and are associated with tumor progression.<sup>28</sup> These data suggest that the differentiation of protumor SPM towards LPM could decrease tumor progression.

Because CCAAT/enhancer binding protein  $\beta$  (C/EBP $\beta$ ) is a critical transcription factor for SPM-to-LPM differentiation<sup>27</sup> and C/EBP $\beta$  cooperate with peroxisome proliferator-activated receptor  $\gamma$  (PPAR $\gamma$ ) in cellular differentiation,<sup>29,30</sup> PPAR $\gamma$  activation could promote the antitumor response by increasing the transition of SPM towards LPM. Furthermore, since PPAR $\gamma$  can increase GATA6 expression in allergic conditions,<sup>31</sup> targeting PPAR $\gamma$  could also directly impact the SPM/LPM balance that allows LPM maintenance in the peritoneum.

PPAR $\gamma$  is activated by a range of synthetic and endogenous ligands derived from the arachidonic acid metabolism. Among these ligands, 15-deoxy- $\Delta^{12,14}$ -PGJ<sub>2</sub>, metabolized through the COX1/COX2 cyclooxygenases, and 12-hydroxyicosatetraenoic acids (HETEs) and 15-HETEs, metabolized through 5-lipoxygenases and 12-lipoxygenases or 15-lipoxygenases, respectively, are essential for PPAR $\gamma$  endogenous activation.<sup>32</sup> The 15-HETE/PPAR axis was identified as a critical component of alternative polarization of macrophages. This activation was responsible for fungicidal and antitumor responses of macrophages through the arginase overexpression and C-type lectin receptor (CLR)-mediated reactive oxygen species (ROS) production.<sup>33,34</sup>

Several lines of evidence support that 15-lipoxygenase expression and 15(S)-HETE production are lost in several high-grade epithelial neoplasia.<sup>35–37</sup> Despite the

controversy over the influence of PPAR $\gamma$  in colorectal cancer, PPAR $\gamma$  has consistently been shown as a tumor suppressor in other types of cancer, such as mammary, ovarian and skin cancer.<sup>38–41</sup> Consistently, low expression of PPAR $\gamma$  in epithelial ovarian cancer tissues is associated with poorer survival of patients with OVAD.<sup>42</sup> Thus, targeting PPAR $\gamma$  in cancer treatment remains an important research area.<sup>43–47</sup>

In this study, we show that the antitumor activity of 15(S)-HETE in a mouse model of OVAD is mediated through PPAR $\gamma$  of macrophages. We also demonstrate that 15(S)-HETE treatment orients the peritoneal macrophage population balance towards LPM by promoting SPM-to-LPM differentiation and LPM peritoneal residence. Importantly, 15(S)-HETE promotes the differentiation and the peritoneal attachment of human ovarian TAMs and attenuates their immunosuppressive properties. Therefore, our study identifies PPAR $\gamma$  as a potential therapeutic target to restrain OVAD growth.

## METHODS

### Cell culture

The murine ovarian cancer cell line ID8 (kindly provided by K Roby, University of Kansas, Kansas City, Kansas, USA)<sup>48</sup> was cultured in Dulbecco's modified Eagle's medium (Invitrogen), supplemented with L-glutamine (Invitrogen), penicillin, streptomycin (Invitrogen) and 10% heat-inactivated fetal calf serum (FCS). For bioluminescence quantification, ID8 cells were transfected with a lentiviral vector encoding firefly luciferase under the control of the cytomegalovirus (CMV) promoter as well as a puromycin selection gene (Addgene) as previously described in a study conducted by Couderc *et al.*<sup>49</sup>

### Mice

All mouse experiments were performed according to protocols approved by the institutional ethics committee (CEEA122) with permit number 6555–2016082912056664v3 in accordance with European legal and institutional guidelines (2010/63/UE) for the care and use of laboratory animals. Wild-type (CD45.1 and CD45.2) C57BL/6 mice were purchased from Janvier Labs. PPAR $\gamma^{M-/-}$  mice have been described and the corresponding floxed littermates were used as controls throughout all the experiments.<sup>50 51</sup> RAG-2 $^{-/-}$  mice were purchased from Envigo.

### Murine ovarian cancer model, 15(S)-HETE treatment and adoptive transfer

ID8 cells expressing luciferase ( $5.10^6$  cells/mouse in 200  $\mu$ L PBS) were administered intraperitoneally (i.p.) into 8–9 weeks old syngeneic C57BL/6 female mice (n=6 per group). This ID8 orthotopic mouse model is a well-established experimental model of end-stage epithelial ovarian carcinoma.<sup>52</sup>

Mice were injected i.p. with 15(S)-HETE (Cayman Chemicals) (12  $\mu$ g/mouse, 1 day after ID8 injection and

then every 4 days), with rosiglitazone (Cayman Chemicals) (56  $\mu$ g/mouse, 1 day after ID8 injection and then every 4 days) or, for control groups, with saline solution (NaCl 0.9%). For depleting macrophages, mice were i.p. injected liposomal clodronate (Xygieia Bioscience, 250  $\mu$ g per mouse) 1 day before tumor cell injection and then every 4 days; control groups received control liposome. At 7, 18, 35 or 50 days after ID8 cell injection, mice were euthanized using CO<sub>2</sub> asphyxia.

Bone marrow cells were collected from CD45.1 C57BL/6 mice paw bones, femurs and tibias in PBS and filtered. Red blood cells were lysed and bone marrow monocytes were sorted by negative selection on MACS columns (Monocyte Isolation Kit (BM) mouse, Miltenyi Biotec). Bone marrow monocytes were injected in the retro-orbital vein of CD45.2 mice ( $5.10^5$  cells/mouse) 11 days after ID8 injection and mice were i.p. treated with 200  $\mu$ L of BrdU (10 mg/mL) 3 hours before being euthanized using CO<sub>2</sub> asphyxia 18 days after ID8 injection.

### Assessment of tumor progression

Mice were monitored daily for signs of tumor progression and evaluation of body weight. For in vivo imaging study, mice were anesthetized by isoflurane, i.p. injected with luciferin (150  $\mu$ g/g body weight), and imaged 6 min later with 30 s exposure length using in vivo imaging system (PerkinElmer). The luminescent images were analyzed using Living Image V.4.4 software.

After mice euthanasia, peritoneal cells were removed aseptically and supernatants (ascites fluids) were collected for cytokines measurement. Luciferase activity was measured on peritoneal cell samples and on diaphragm and peritoneal membrane with a luminometer (EnVision, PerkinElmer). The volume of ascites fluid was determined by aspirating with a needle and syringe.

### Macrophage cytotoxicity assay

Macrophages in ascites of mice were separated from other peritoneal cells by a Percoll density gradient (Percoll, Sigma-Aldrich) followed by 2 hours of adhesion. Macrophages were co-cultured 72 hours with ID8 cells then the number of viable ID8 cells was evaluated by measuring the luciferase activity 10 min after D-Luciferin addition (Caliper, 9  $\mu$ g/mL) with a luminometer.

### Flow cytometry

After mice euthanasia, peritoneal cells were harvested, centrifuged and red blood cells were lysed with ammonium-chloride-potassium (ACK) lysing buffer.<sup>53</sup> Omental cells were harvested after tissue digestion.<sup>53</sup> All analyses were gated on viable cells after a Live/Dead Staining (Molecular Probes LIVE/DEAD Fixable Violet Dead Cell Stain Kit, Life Technologies).

For lymphocyte population infiltration/activation and T helper 1 (Th1)/Th2 profile studies, peritoneal cells were labeled with the following antibodies: CD3-PE, CD4-VioBrightFITC, CD8-VioGreen, CD25-PEVio770,

NK1.1-PerCPVio700, CD19-APCVio700, CD183-APC and Foxp3-Vio667 (Miltenyi Biotec).

Peritoneal and omental macrophages were analyzed by surface expressed MHCII and F4/80 detection using MHCII-Vioblue and F4/80-APC (Miltenyi Biotec), respectively, in CD45<sup>+</sup> (VioGreen, Miltenyi Biotec) and CD11b<sup>+</sup> (FITC, Miltenyi Biotec) cells. To identify the origin of different populations, CD45.2-PerCPVio770 and CD45.1-PE antibodies (Miltenyi Biotec) were used. Finally, cells were washed and resuspended in 300  $\mu$ L PBS 1% heat-inactivated FCS. To analyze cells proliferation, peritoneal macrophage populations were stained with anti-BrdU antibody (PE, Miltenyi Biotec).

Human ascitic macrophage populations were analyzed by surface expressed markers CD14 and CD16 using CD14-PerCPVio700 (Miltenyi Biotec) and CD16-VioBright R720 (Miltenyi Biotec) antibodies, respectively.

Appropriate fluorochrome-matched isotype antibodies were used to determine non-specific background staining. All stainings were performed on 100  $\mu$ L of PBS 1% heat-inactivated FCS. A population of 10,000 cells was analyzed for each data point. All analyses were done in a BD Fortessa flow cytometer with Diva software. A multiplex bead-based immunoassay was used (BioLegend, LEGENDplex Mix and Match System) for ascites cytokine measurement. The gating strategies were detailed in online supplemental figures 4 and 5.

### Image flow cytometry

After mice euthanasia, peritoneal cells were harvested, centrifuged and red blood cells were lysed with ACK lysing buffer. Peritoneal macrophage population was analyzed by surface expressed MHCII and F4/80 detection, respectively, using MHCII-PE (Miltenyi Biotec) and F4/80-PECy7 (eBiosciences) antibodies. Cells were washed, permeabilized then incubated with 4',6-diamidino-2-phenylindole (DAPI) for nucleus staining, anti-PPAR $\gamma$  antibody (AF680, Bioss) and anti-C/EBP $\beta$  (FITC, Biorbyt) or anti-GATA6 (FITC, Biorbyt) antibodies. Then, cells were washed and resuspended in 300  $\mu$ L PBS<sup>-/-</sup> 1% heat-inactivated FCS. Appropriate fluorochrome-matched isotype antibodies were used to determine non-specific background staining. All stainings were performed on 100  $\mu$ L of PBS<sup>-/-</sup> 1% heat-inactivated FCS. Individual cell images were acquired using IDEAS software (Amnis Merck Millipore, Billerica, Massachusetts, USA) on a 3-laser 6-channel imaging flow cytometer (Image Stream X Mark II, Amnis Merck Millipore) with  $\times 40$  magnification. For each data file, at least 50,000 single cells were acquired, debris and doublets were excluded based on their area and aspect ratio. Single-stain controls were acquired (all channels on, no brightfield and no side scatter image), a compensation matrix was calculated and then applied to the data files using IDEAS software (Amnis Merck Millipore). Briefly, focus cells were identified using the gradient root mean squared (RMS) feature of the brightfield channel (Ch04). Single cells were then identified from debris and

cell clusters using a plot of aspect ratio versus area of the brightfield channel.

### Peritoneal macrophage and lymphocyte cell sorting

Peritoneal cells were stained with the following antibodies: CD45-APCy7 (BioLegend), F4/80-APC, MHCII-Vioblue and CD3-PE (Miltenyi Biotec). The two peritoneal macrophage populations and lymphocytes were sorted with a BD Influx cell sorter.

### Macrophage ex vivo treatment

After mice euthanasia, peritoneal cells were harvested, centrifuged and red blood cells were lysed with ACK lysing buffer, then allowed to adhere for 2 hour. After washing, macrophages isolated from tumor-bearing mice were treated or not with 15(S)-HETE (Cayman Chemicals, 1  $\mu$ M) or rosiglitazone (Cayman Chemicals, 5  $\mu$ M) for 48 hours then lysed and used for real-time PCR.

### Isolation and treatment of macrophages isolated from patients' ascites

Ascitic fluids from individuals with ovarian cancer were collected from chemotherapy-naïve patients who underwent a tumor surgical resection at the Claudius Regaud Institute (IUCT Oncopole, Toulouse, France). Ascitic fluids were obtained aseptically in heparinized vacuum bottles from patients with pathologically confirmed OVAD. Appropriate informed consents were obtained from all cases. Fluids were passed through a 100  $\mu$ M filter to obtain a single cell suspension. TAMs were isolated from patients' ascites with a Percoll density gradient as described previously in a study conducted by Hamburger *et al.*<sup>54</sup>

The fraction containing macrophages was allowed to adhere for 2 hours and then treated or not with 15(S)-HETE (Cayman Chemicals, 1  $\mu$ M) for 48 hours then lysed and used for real-time PCR.

### Reverse transcription and real-time PCR

Messenger RNA (mRNA) was isolated using the RNAqueous-Micro Total RNA Isolation Kit (Thermo Fisher) following the manufacturer's protocol and complementary DNA (cDNA) was synthesized according to the manufacturer's recommendations (Verso Kit, Thermo Electron). Real-time quantitative polymerase chain reaction (RT-qPCR) was performed in a total volume of 10  $\mu$ L with 60 cycles of 10s at 95°C, 10s at 60°C and 10s at 72°C using a LightCycler 480 system and LightCycler SYBR Green I Master (Roche Diagnostics). The primers (at a final concentration of 5  $\mu$ M) were designed with the software Primer 3. The glyceraldehyde-3-phosphate dehydrogenase (*Gapdh*) mRNA was used as the invariant control. Serially diluted samples of pooled cDNA were used as external standards in each run for the quantification. Primer sequences are listed in online supplemental table 1.

## Statistical analysis

For each experiment, the data were subjected to one-way analysis of variance followed by the means multiple comparison method of Bonferroni-Dunnnett.  $P$  value  $< 0.05$  was considered as the level of statistical significance.

## RESULTS

### 15(S)-HETE treatment inhibits OVAD progression in vivo through macrophages

We evaluated the effect of 15(S)-HETE on the tumor burden using an ovarian epithelial tumor murine model.<sup>48</sup> ID8 cells expressing the firefly luciferase gene (*luc2*) were intraperitoneally injected into syngeneic female C57BL/6 mice, which resulted in peritoneal

carcinomatosis, particularly on peritoneal membrane and diaphragm, and extensive hemorrhagic ascites fluid production after 18 days (figure 1A). The mice present signs similar to advanced-stage 3 epithelial ovarian cancer, including the development of ascites in the peritoneal cavity and secondary lesions on the peritoneum walls and other organs within the peritoneal cavity.<sup>52</sup>

Treating ID8 tumor-bearing mice with 15(S)-HETE significantly decreased tumor-derived bioluminescence in the abdomen, the peritoneal membrane, the diaphragm and the ascites (figure 1B–E) as well as the ascites volume and the weight gain (figure 1F).

To investigate whether 15(S)-HETE treatment impacted macrophage cytotoxic activity, we evaluated the

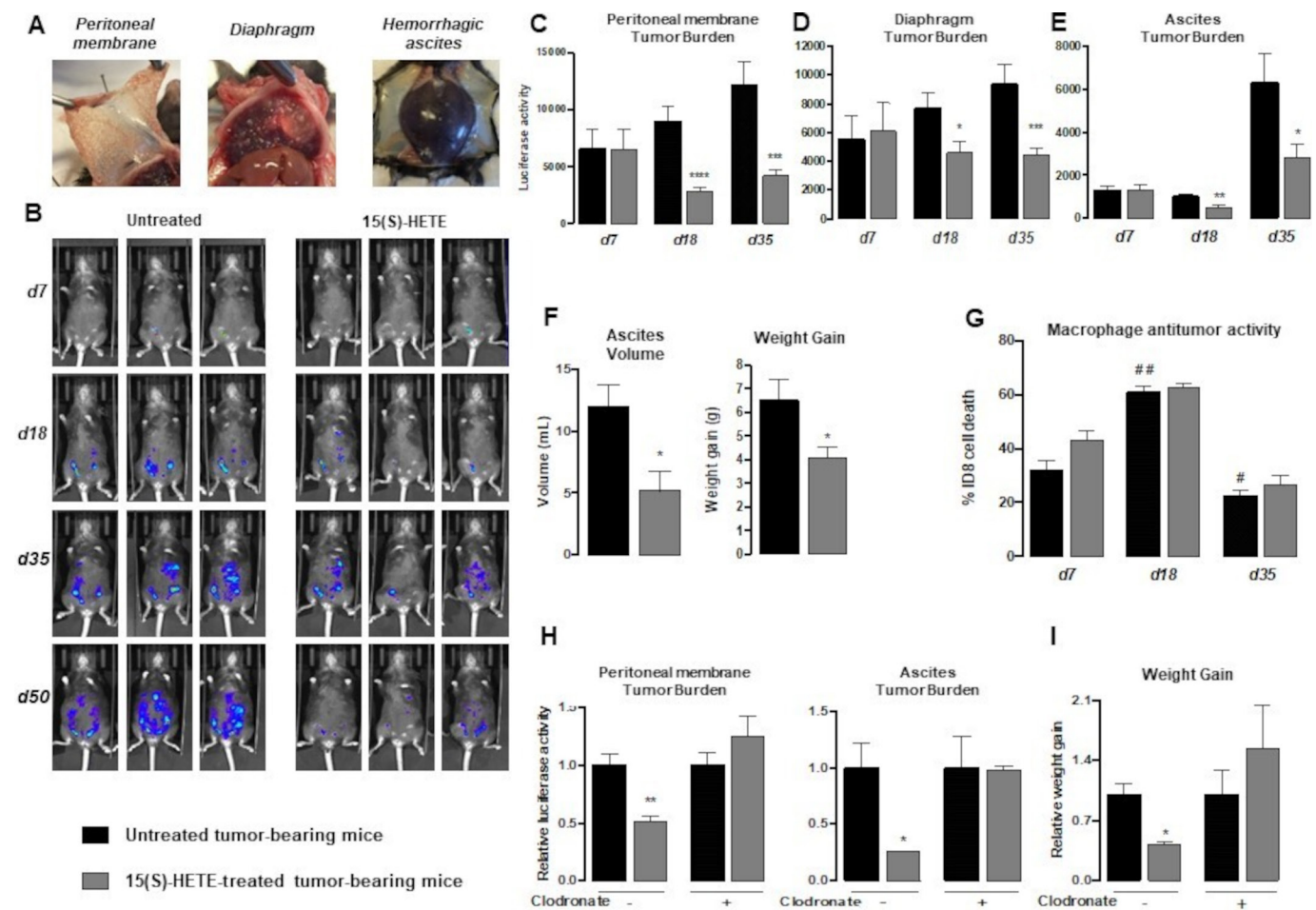


**Figure 1** In vivo 15(S)-HETE treatment inhibits OVAD progression through macrophages. (A) Photographs of tumor burden in peritoneal membrane, diaphragm and ascites of untreated tumor-bearing mice 50 days post-tumor cells injection. (B–E) In vivo imaging (B) and quantification of peritoneal membrane (C), diaphragm (D) and ascites (E) tumor burdens by bioluminescence in untreated or 15(S)-HETE-treated mice at days 7, 18, 35 and 50 post-ID8 implantation. (F) Ascites volume and weight gain of untreated and 15(S)-HETE-treated mice 50 days post-tumor cells injection. (G) Cytotoxic activity of peritoneal macrophages collected from the ascites of untreated and 15(S)-HETE-treated mice determined by the quantification of bioluminescence intensity after 72 hours of co-culture with ID8-Luc tumor cells. (H–I) Peritoneal membrane and ascites tumor burden quantified by bioluminescence (H) and weight gain (I) in mice without or with depletion of macrophages were evaluated at day 35 post-ID8 implantation. Tumor burden and weight gain data are expressed as fold induction relative to corresponding untreated ID8 tumor-bearing mice. Results correspond to mean  $\pm$  SEM ( $n=6$  per group) and are representative of at least three independent experiments.  $*p < 0.05$ ,  $**p < 0.01$ ,  $***p < 0.001$  and  $****p < 0.0001$  compared with respective untreated ID8 tumor-bearing mice.  $\#p < 0.05$  and  $##p < 0.01$  compared with untreated mice at day 7. HETE, hydroxyeicosatetraenoic acid; OVAD, ovarian adenocarcinoma

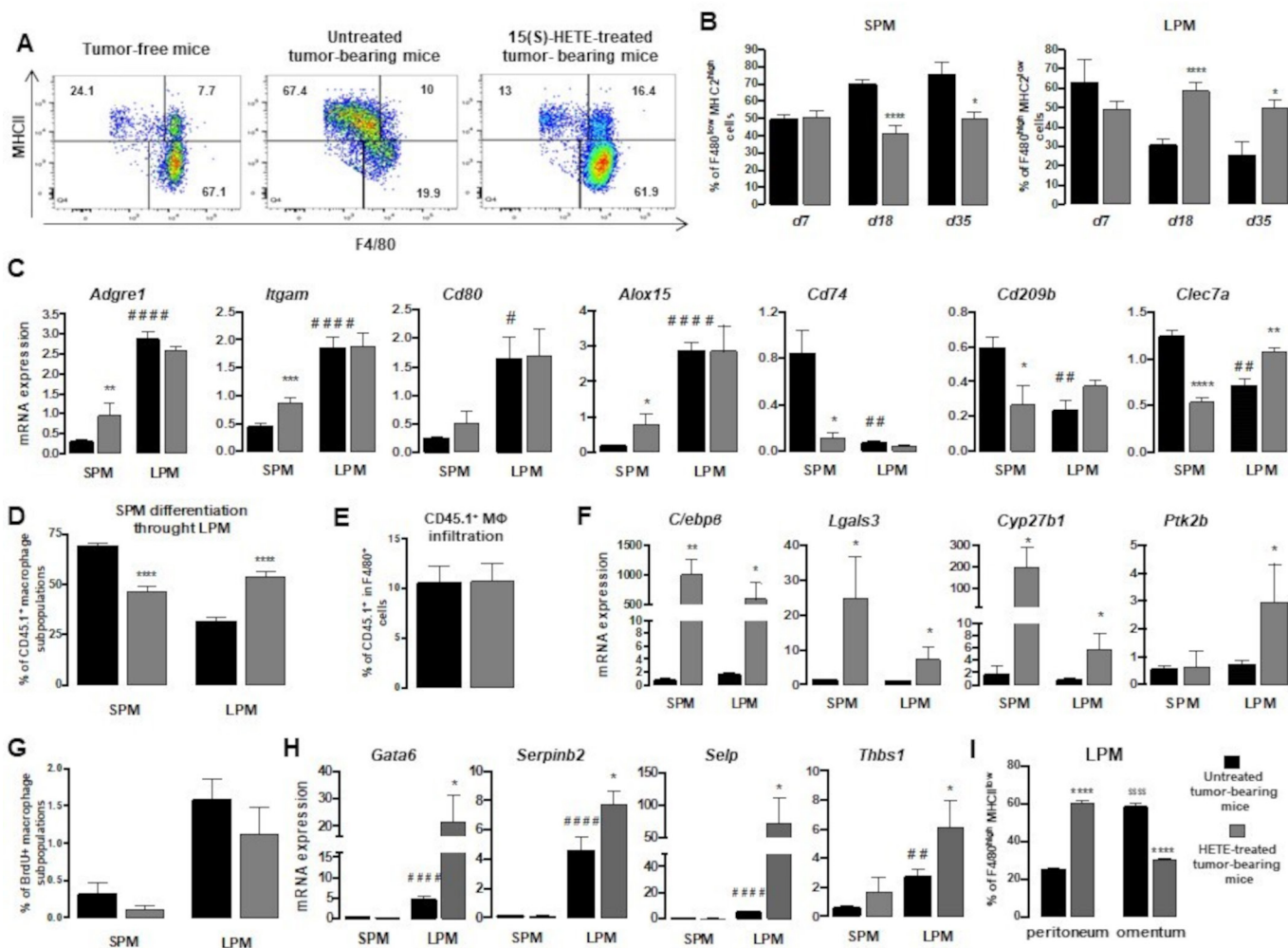


**Figure 2** 15(S)-HETE treatment promotes the differentiation of SPM towards LPM and the LPM maintenance in the peritoneum. (A) Dot-plot showing SPM (F4/80<sup>low</sup> MHCII<sup>high</sup>) and LPM (F4/80<sup>high</sup> MHCII<sup>low</sup>) day 18 post-ID8 injection. (B) Quantification of SPM and LPM in the F4/80<sup>+</sup> MHCII<sup>+</sup> population at days 7, 18 and 35 post-tumor cell injection. (C) Expressions of differentiation marker genes in SPM and LPM sorted at day 18 post-ID8 injection. (D–E) SPM-to-LPM differentiation in CD45.1<sup>+</sup> monocytes-transplanted CD45.2<sup>+</sup> host tumor-bearing mice treated or not with 15(S)-HETE at day 11-post tumor cells injection (D) and CD45.1<sup>+</sup> macrophage infiltration (E) were quantified by flow cytometry using F4/80, MHCII, CD45.1 and CD45.2 markers. (F) Expressions of SPM-to-LPM differentiation marker genes in SPM and LPM sorted at day 18 post-ID8 injection. (G) Tumor bearing mice treated or not with 15(S)-HETE were injected with BrdU 3 hours before euthanasia and BrdU incorporation was assessed by flow cytometry. (H) Expression of peritoneal residency marker genes in SPM and LPM sorted at day 18 post-ID8 injection measured using RT-qPCR. (I) Quantification of LPM in the peritoneum and omentum at day 18 post-tumor cell injection. Results correspond to mean±SEM (n=6 per group) and are representative of at least three independent experiments. \*p<0.05, \*\*p<0.01, \*\*\*p<0.001 and \*\*\*\*p<0.0001 compared with respective untreated ID8 tumor-bearing mice. ##p<0.01 and ###p<0.001 compared with SPM from untreated ID8 tumor-bearing mice. \$\$\$\$p<0.0001 compared with peritoneal LPM from untreated ID8 tumor-bearing mice. HETE, hydroxyeicosatetraenoic acid; LPM, large peritoneal macrophages; mRNA, messenger RNA; OVAD, ovarian adenocarcinoma; RT-qPCR, real-time quantitative polymerase chain reaction; SPM, small peritoneal macrophages.

ability of macrophages from 15(S)-HETE-treated tumor bearing mice to eliminate ID8 tumor cells. At day 35 post ID8 injection, the percentage of ID8 cell death is strongly decreased compared with day 18 post ID8 injection, demonstrating that macrophages isolated from untreated-mice ascites at day 35 post ID8 injection have decreased antitumor activity (figure 1G). 15(S)-HETE-treatment of tumor-bearing mice did not improve the ability of ascites macrophages to kill ID8 cells at days 7, 18 and 35 post ID8 injection (figure 1G), supporting that 15(S)-HETE in vivo

antitumor activity cannot be assigned to an increase of the direct cytotoxic activity of macrophages.

To assess whether macrophages contribute to 15(S)-HETE's antitumor activity, we determined 15(S)-HETE's antitumor activity in tumor bearing mice selectively depleted of macrophages (online supplemental S1). Interestingly, macrophage depletion inhibited 15(S)-HETE-induced antitumor activity (figure 1H) and abrogated the reduced weight gain in 15(S)-HETE-treated mice (figure 1I). These results indicated that the

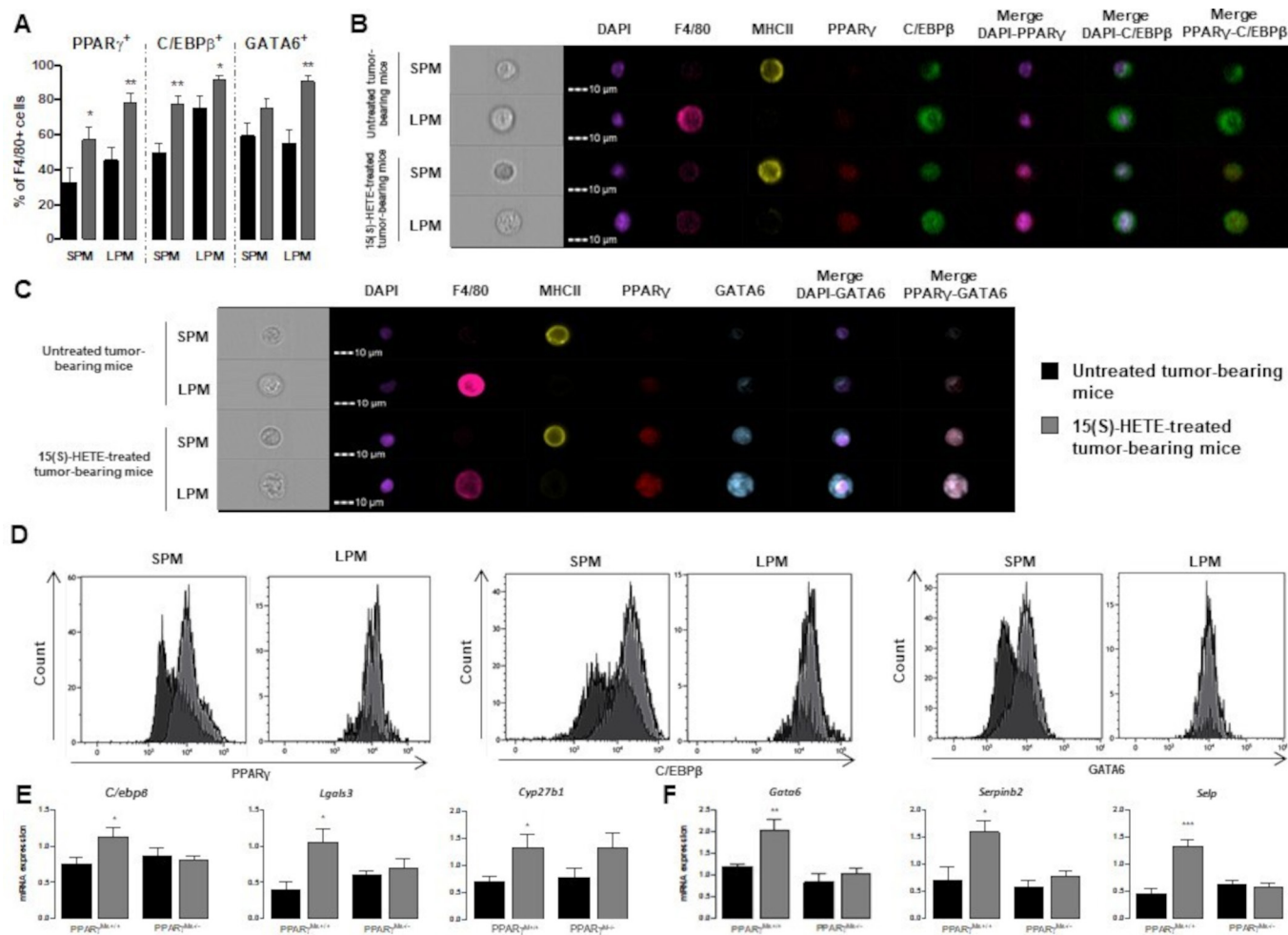


**Figure 3** 15(S)-HETE treatment leads to C/EBP $\beta$  and GATA6 activation through PPAR $\gamma$  in TAMs. (A, B) Percentage of SPM or LPM expressing PPAR $\gamma$ , C/EBP $\beta$  or GATA-6 (A) and visualization of PPAR $\gamma$  and C/EBP $\beta$  and their colocalization on SPM and LPM from untreated or treated tumor-bearing mice by Image StreamX (B). (C) Visualization of PPAR $\gamma$  and GATA-6 and their colocalization on SPM and LPM from untreated or treated tumor-bearing mice by Image StreamX. (D) Quantification of PPAR $\gamma$ , C/EBP $\beta$  and GATA-6 on SPM and LPM from untreated or treated tumor-bearing mice by Image StreamX. (E–F) Macrophages isolated from the ascites of untreated or 15(S)-HETE-treated PPAR $\gamma^{M+/+}$  or PPAR $\gamma^{M-/-}$  tumor-bearing mice were analyzed for expressions of SPM-to-LPM differentiation markers (E) and peritoneal residency markers (F) using RT-qPCR. Results correspond to mean $\pm$ SEM (n=6 per group) and are representative of at least three independent experiments. \*p<0.05, \*\*p<0.01 and \*\*\*p<0.001 compared with respective untreated ID8 tumor-bearing mice. C/EBP $\beta$ , CCAAT/enhancer binding protein  $\beta$ ; HETE, hydroxyeicosatetraenoic acid; LPM, large peritoneal macrophages; mRNA, messenger RNA; PPAR $\gamma$ , peroxisome proliferator-activated receptor  $\gamma$ ; SPM, small peritoneal macrophages; RT-qPCR, real-time quantitative PCR; TAMs, tumor-associated macrophages.

impact of 15(S)-HETE in tumor development is mediated through the macrophages.

### 15(S)-HETE treatment promotes the differentiation of SPM towards LPM and the LPM maintenance in the peritoneum

Based on suggested protumor and proangiogenic properties of SPM in the literature,<sup>28</sup> we investigated the influence of 15(S)-HETE treatment on the LPM/SPM proportion in tumor ascites. As expected, LPM were more abundant than SPM in the peritoneal cavity of tumor-free mice (figure 2A). In tumor bearing mice ascites, the proportion of SPM strongly increased whereas the proportion of LPM decreased (figure 2A,B). 15(S)-HETE treatment restored the LPM/SPM ratio similar to that of tumor-free mice (figure 2A).

SPM had been reported to differentiate into LPM to maintain the resident macrophage proportion during inflammatory situations,<sup>24 27</sup> we therefore evaluated the impact of 15(S)-HETE on SPM conversion towards LPM using established markers<sup>23 24</sup> (figure 2C, online supplemental table 2). As expected, LPM sorted from ascites of untreated tumor-bearing mice expressed high levels of F4/80 (*Adgre1*), CD11b (*Itgam*), CD80 and 12/15-Lox (*Alox15*) and low levels of MHCII (*Cd74*), DC-SIGN (*Cd209b*) and Dectin-1 (*Clec7a*) while SPM showed a F4/80<sup>low</sup> CD11b<sup>low</sup> CD80<sup>low</sup> 12/15-lox<sup>low</sup> MHCII<sup>high</sup> DC-SIGN<sup>high</sup> Dectin-1<sup>high</sup> phenotype (figure 2C, online supplemental table 2). Interestingly, SPM sorted from 15(S)-HETE-treated tumor bearing mice presented an



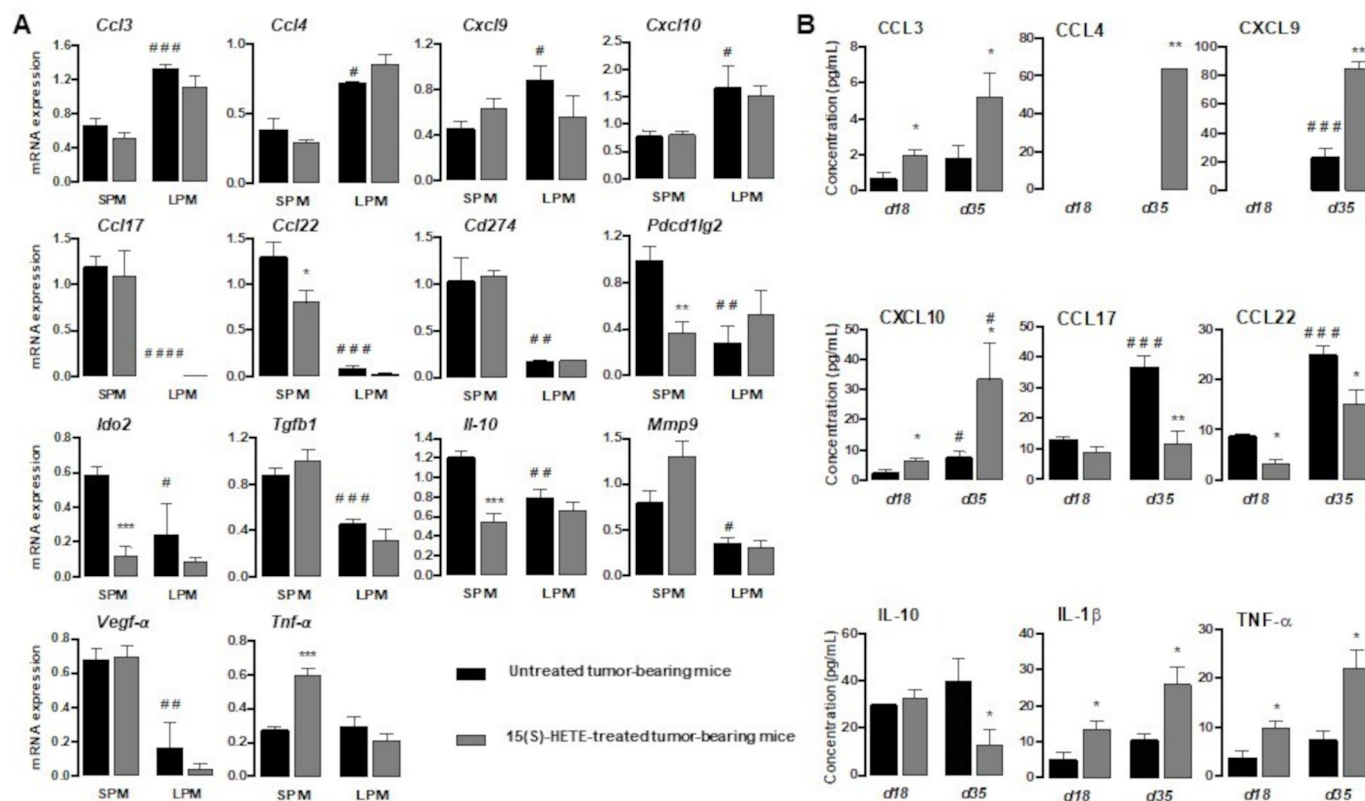


**Figure 4** 15(S)-HETE treatment favors the presence of immunocompetent LPM. (A) SPM and LPM were isolated from the ascites of untreated or 15(S)-HETE-treated mice at day 18 post-ID8 injection using F4/80 and MHCII markers. Their respective phenotypes were determined by gene expression analysis of chemotaxis, immunosuppression, angiogenesis, metastasis factors and of proinflammatory or anti-inflammatory cytokines using RT-qPCR. (B) Protein levels of chemotactic factors and proinflammatory or anti-inflammatory cytokines in tumor ascites at days 7, 18 and 35 post-tumor cell injection were evaluated by flow cytometry. Results correspond to mean±SEM (n=6 per group) and are representative of at least three independent experiments. \*p<0.05, \*\*p<0.01 and \*\*\*p<0.001 compared with respective untreated ID8 tumor-bearing mice. #p<0.05, ##p<0.01, ###p<0.001 and ####p<0.0001 compared with SPM from untreated ID8 tumor-bearing mice. HETE, hydroxyeicosatetraenoic acid; IL, interleukin; LPM, large peritoneal macrophages; mRNA, messenger RNA; RT-qPCR, real-time quantitative PCR; SPM, small peritoneal macrophages; TNF, tumor necrosis factor.

intermediate phenotype characterized by an induction of genes highly expressed in LPM and a decrease of genes weakly expressed in LPM. These results suggest that 15(S)-HETE treatment promotes the differentiation of SPM into LPM in OVAD bearing mice.

To further confirm the impact of 15(S)-HETE on the differentiation of SPM towards LPM, we adoptively transferred bone marrow monocytes from CD45.1 mice to tumor-bearing CD45.2 mice, treated or not with 15(S)-HETE. Flow cytometry analysis of peritoneal cells showed that 15(S)-HETE treatment decreased the percentage of CD45.1<sup>+</sup> SPM and increased the percentage of CD45.1<sup>+</sup> LPM in tumor-bearing mice (figure 2D), without significantly affecting the total recruited CD45.1 cells (figure 2E). These results confirmed that SPM could differentiate into LPM in an ovarian cancer model and showed that 15(S)-HETE potentiated this differentiation. C/EBPβ is a key transcription factor of the SPM-to-LPM differentiation,<sup>27</sup> we therefore evaluated the expression of C/EBPβ and its target genes. SPM and LPM from untreated tumor-bearing mice expressed low levels of C/

EBPβ (*Cebpb*), *Mac2* (*Lgals3*), 1α-hydroxylase (*Cyp27b1*) and *Pyk2* (*Plk2b*) (figure 2F, online supplemental table 2). 15(S)-HETE treatment increased mRNA levels of *Cebpb*, *Lgals3*, and *Cyp27b1* in both SPM and LPM and increased *Plk2b* expression in LPM (figure 2F, online supplemental table 2). Altogether, these results support that 15(S)-HETE treatment promotes SPM-to-LPM differentiation through C/EBPβ expression and activation in ovarian tumor-bearing mice.

LPM can self-renew in the peritoneum.<sup>24</sup> However, 15(S)-HETE treatment did not enhance LPM proliferation measured by BrdU incorporation (figure 2G). The reduced SPM/LPM ratio on 15(S)-HETE treatment could be also the consequence of decreased MDR.<sup>25</sup> Thus, the expression and the activation of GATA6, a transcription factor for LPM-specific genes involved in their peritoneal adherence,<sup>26</sup> were evaluated. As expected, the expression of GATA6 and its target genes were observed only in LPM (figure 2H, online supplemental table 2). The 15(S)-HETE treatment strongly increased LPM expression of *Gata6*, *Serp1nb2*, *Selp* (CD62p) and *Thbs1* (figure 2H,

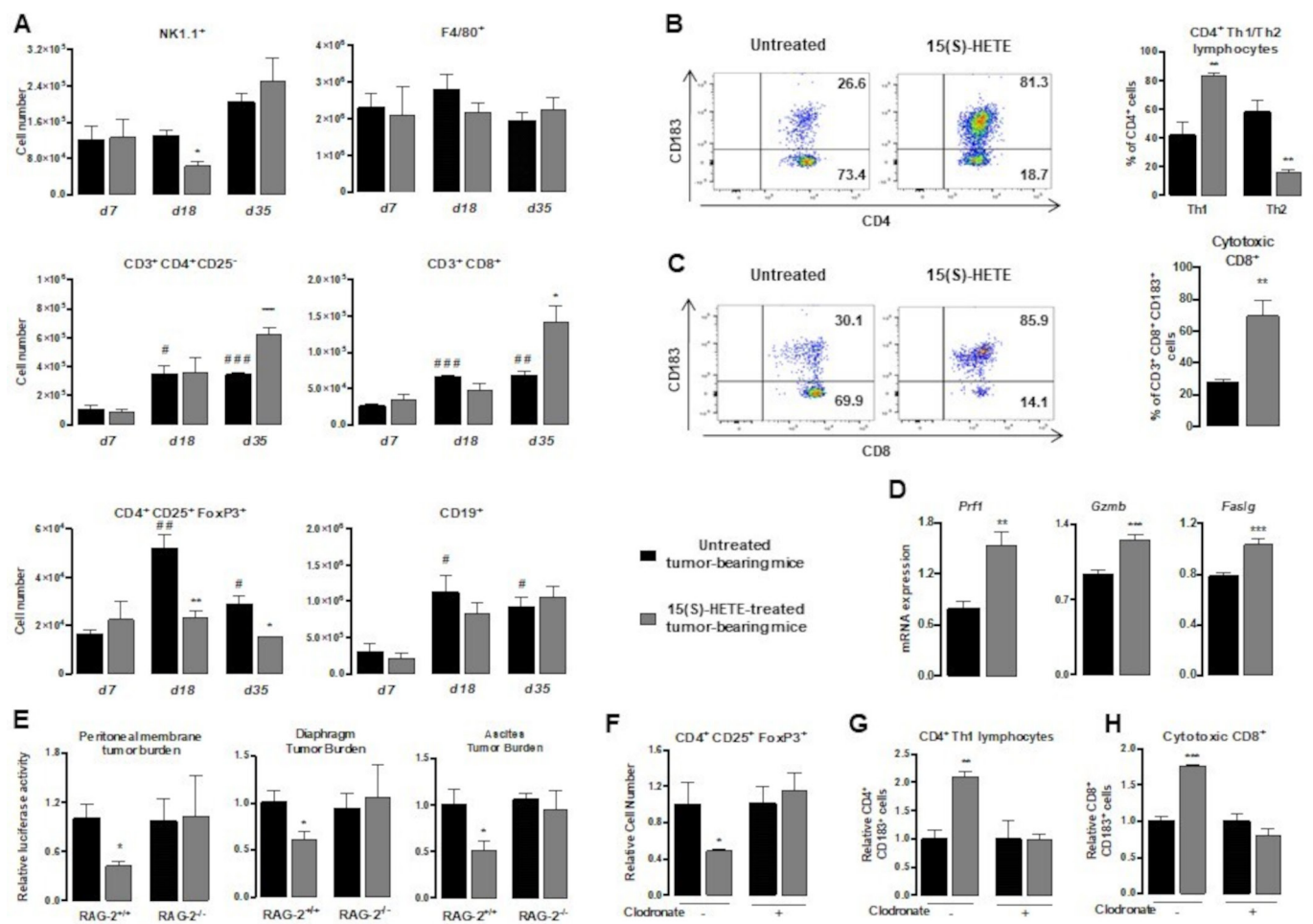


**Figure 5** 15(S)-HETE treatment improves the effector/regulatory T-cell ratio in tumor ascites through a mechanism dependent on macrophages. (A) Macrophage and lymphocyte in ascites of untreated or 15(S)-HETE-treated mice at days 7, 18 and 35 post-ID8 cell injection were evaluated by flow cytometry after staining with appropriate markers. (B) Percentages of Th1/Th2 CD4<sup>+</sup> lymphocytes in the CD4<sup>+</sup> population at day 35 post-ID8 injection were evaluated by flow cytometry after staining with CD183 antibody. (C) The per cent of cytotoxic CD8<sup>+</sup> lymphocytes in CD8<sup>+</sup> population at day 35 post-ID8 injection was evaluated by flow cytometry after staining with CD183 antibody. (D) Lymphocytes activation at day 35 post-ID8 injection evaluated by analyzing *Prfl*, *Gzmb* and *Faslg* expression using RT-qPCR. (E) Wild-type (RAG-2<sup>+/+</sup>) or RAG-2<sup>-/-</sup> mice were injected intraperitoneally with 5×10<sup>6</sup> ID8-Luc2 cells then treated or not with 15(S)-HETE every 4 days. Peritoneal membrane, diaphragm and ascites tumor burdens were evaluated at day 35 post-tumor cell injection by bioluminescence quantification. Tumor burden data are expressed as fold induction relative to the corresponding untreated ID8 tumor-bearing mice. (F–H) Tregs infiltration (F), the per cent of Th1 CD4<sup>+</sup> lymphocytes (G) and the per cent of cytotoxic CD8<sup>+</sup> lymphocytes (H) in macrophage-depleted mice were evaluated by flow cytometry with appropriate markers at day 35 post-ID8 cells injection. Data are expressed as fold induction relative to the corresponding untreated ID8 tumor-bearing mice. Results correspond to mean±SEM (n=6 per group) and are representative of at least three independent experiments. \*p<0.05, \*\*p<0.01 and \*\*\*p<0.001 compared with respective untreated ID8 tumor-bearing mice. #p<0.05, ##p<0.01 and ###p<0.001 compared with untreated mice at day 7. HETE, hydroxyeicosatetraenoic acid; NK, natural killer; RT-qPCR, real-time quantitative PCR; Th1, T lymphocyte regulator; Treg, regulatory T cell.

online supplemental table 2). These data suggest that 15(S)-HETE treatment could inhibit LPM migration from the peritoneum toward the omentum. The HETE-induced LPM peritoneal residence was confirmed by a higher frequency of LPM in the peritoneum associated with a lower proportion of LPM in the omentum (figure 2I). Thus, these data suggest that the increase of LPM following 15(S)-HETE treatment is associated with both SPM-to-LPM differentiation and a LPM residency in the peritoneal cavity.

### PPAR $\gamma$ mediates 15(S)-HETE treatment-induced C/EBP $\beta$ and GATA6 activation

To examine the role of PPAR $\gamma$  in 15(S)-HETE-induced differentiation of SPM toward LPM through C/EBP $\beta$ , we investigated PPAR $\gamma$  and C/EBP $\beta$  nuclear and cytoplasmic localization in SPM and LPM from tumor-bearing mice by image streamX. The 15(S)-HETE treatment increased PPAR $\gamma$ <sup>+</sup> and C/EBP $\beta$ <sup>+</sup> cells proportions in SPM and LPM (figure 3A–D). The 15(S)-HETE induced PPAR $\gamma$  and C/EBP $\beta$  nuclear localization in SPM and LPM (figure 3B,

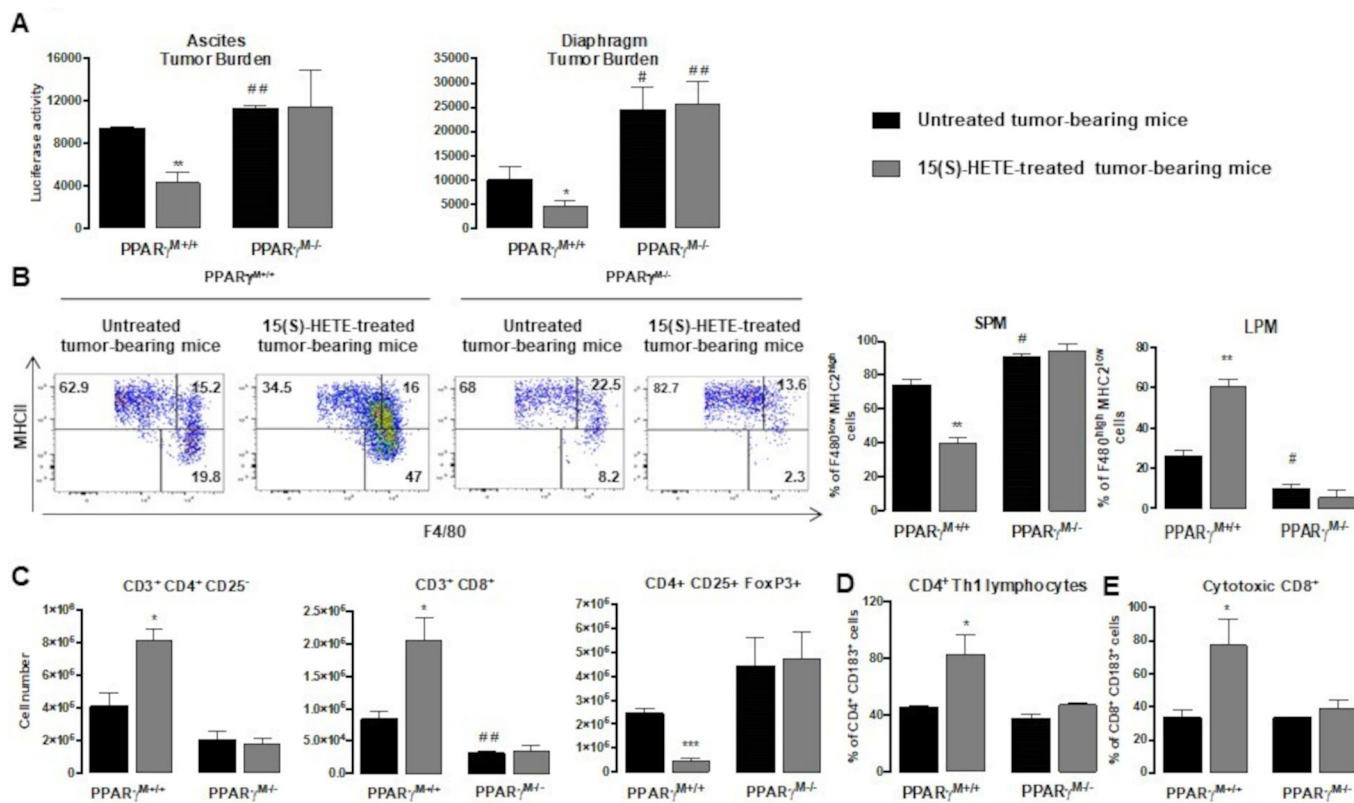


**Figure 6** The antitumor activity of 15(S)-HETE is mediated by PPAR $\gamma$  in macrophages. (A) Ascites and diaphragm tumor burdens were quantified by bioluminescence at day 35 post-tumor cell injection. (B) Dot-plot and histogram quantification of SPM and LPM in F4/80<sup>+</sup> MHCII<sup>+</sup> population at day 35 post-tumor cell injection after F4/80 and MHCII staining. (C) CD4<sup>+</sup>, CD8<sup>+</sup> and Tregs infiltrations evaluated by flow cytometry. (D–E) Percentages of Th1 CD4<sup>+</sup> lymphocytes in CD4<sup>+</sup> population (D) and cytotoxic CD8<sup>+</sup> lymphocytes in CD8<sup>+</sup> population (E) were evaluated by flow cytometry with appropriate markers at day 35 post-ID8 cells injection. Results correspond to mean $\pm$ SEM (n=6 per group) and are representative of at least three independent experiments. \*p<0.05, \*\*p<0.01 and \*\*\*p<0.001 compared with respective untreated ID8 tumor-bearing mice. #p<0.05 and ##p<0.01 compared with PPAR $\gamma^{M+/+}$  untreated mice. HETE, hydroxyeicosatetraenoic acid; LPM, large peritoneal macrophages; PPAR $\gamma$ , peroxisome proliferator-activated receptor  $\gamma$ ; SPM, small peritoneal macrophages; Th1, T lymphocyte regulator; Treg, regulatory T cell.

online supplemental S2, merge DAPI/PPAR $\gamma$  and DAPI/C/EBP $\beta$ ) and PPAR $\gamma$  and C/EBP $\beta$  colocalization in SPM and LPM (figure 3B, merge PPAR $\gamma$ /C/EBP $\beta$ ). Moreover, 15(S)-HETE increased PPAR $\gamma$  and C/EBP $\beta$  protein levels both in SPM and LPM (figure 3C,D, online supplemental S2).

We next evaluated the involvement of the PPAR $\gamma$ -GATA6 axis in the 15(S)-HETE-induced macrophage peritoneal retention in tumor-bearing mice. Although, in LPM, 15(S)-HETE increased the GATA6<sup>+</sup> cells proportion, GATA6 protein level was not changed (figure 3A–D). In SPM only the GATA6 protein level was augmented following 15(S)-HETE treatment (figure 3A–D), indicating that 15(S)-HETE influence macrophage peritoneal retention through GATA6 by increasing its expression in SPM and the number of GATA6<sup>+</sup> cells in LPM. Moreover, 15(S)-HETE induced PPAR $\gamma$  and GATA6 nuclear localization in SPM and LPM (figure 3C, 2online supplemental S2, merge DAPI/GATA6) and PPAR $\gamma$  and GATA6 colocalization in SPM and LPM (figure 3C, online supplemental S2, merge PPAR $\gamma$ /GATA6).

To validate the role of PPAR $\gamma$  in C/EBP $\beta$  and GATA6 activation, we assessed mRNA levels of their target genes and of *Cebpb* and *Gata6* in tumor bearing PPAR $\gamma^{M-/-}$  mice, in which the PPAR $\gamma$  gene (*Pparg*) was selectively disrupted in myeloid-derived cells. The 15(S)-HETE treatment increased the expression of *Cebpb*, *Gata6* and their target genes in macrophages from PPAR $\gamma^{M+/+}$  tumor-bearing mice (figure 3E–F), as expected, but not in macrophages from PPAR $\gamma^{M-/-}$  tumor-bearing mice.

Taken together, these results demonstrate that C/EBP $\beta$  and GATA6 play a central role in SPM-to-LPM differentiation and suggest their involvement in LPM peritoneal residence through PPAR $\gamma$  activation following 15(S)-HETE treatment during OVAD.

### 15(S)-HETE treatment favors the presence of antitumor LPM, which contributes to counteracting cancer immunosuppression

To investigate LPM's potential antitumor phenotype, we evaluated mRNA levels of representative markers of immunity/tolerance balance in SPM and LPM in ascites

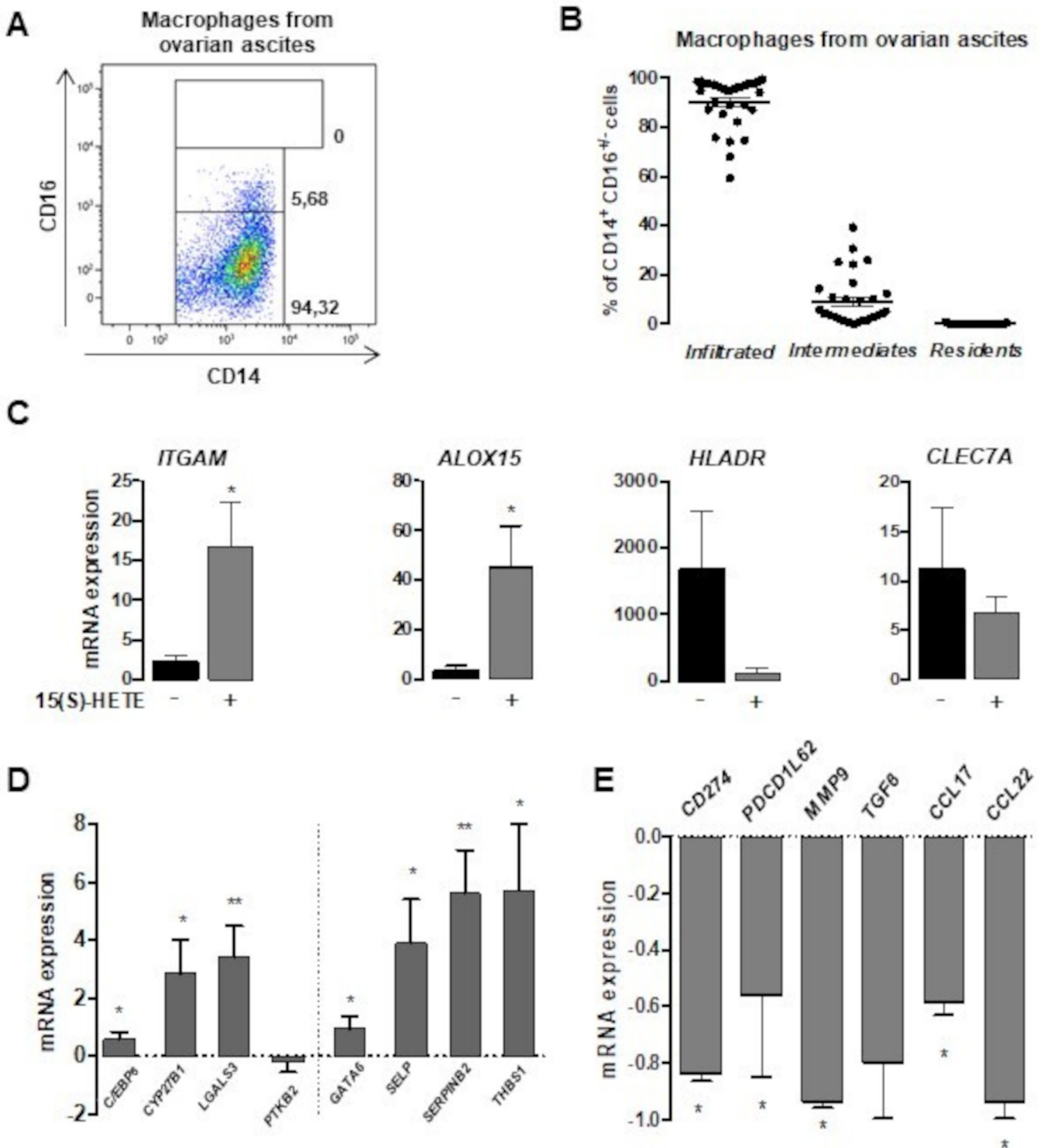


**Figure 7** 15(S)-HETE promotes the differentiation, the peritoneal attachment and attenuates immunosuppressive properties of human ovarian TAMs. (A–B) A representative dot-plot (A) and histogram quantification (B) of Infiltrated macrophages ( $CD14^{inter} CD16^{low}$ ), Intermediate macrophages ( $CD14^{inter} CD16^{inter}$ ) and resident macrophages ( $CD14^{high} CD16^{high}$ ) in the  $CD14^{+} CD16^{+/-}$  population of peritoneal macrophages ( $n=31$  patients). (C–E) Peritoneal macrophages treated or not with 15(S)-HETE ( $1 \mu M$ ) for 48 hours and gene expressions of SPM and LPM differentiation markers (C), factors involved in SPM-to-LPM differentiation and LPM residency (D) and in immunosuppression and metastasis (E) were evaluated by RT-qPCR. Results are expressed as fold induction relative to untreated TAM and correspond to mean  $\pm$  SEM of TAMs isolated from 16 patients. \* $p < 0.05$  and \*\* $p < 0.01$  compared with the respective untreated tumor-associated macrophages. HETE, hydroxyeicosatetraenoic acid; LPM, large peritoneal macrophages; mRNA, messenger RNA; RT-qPCR, real-time quantitative PCR; SPM, small peritoneal macrophages; TAMs, tumor-associated macrophages.

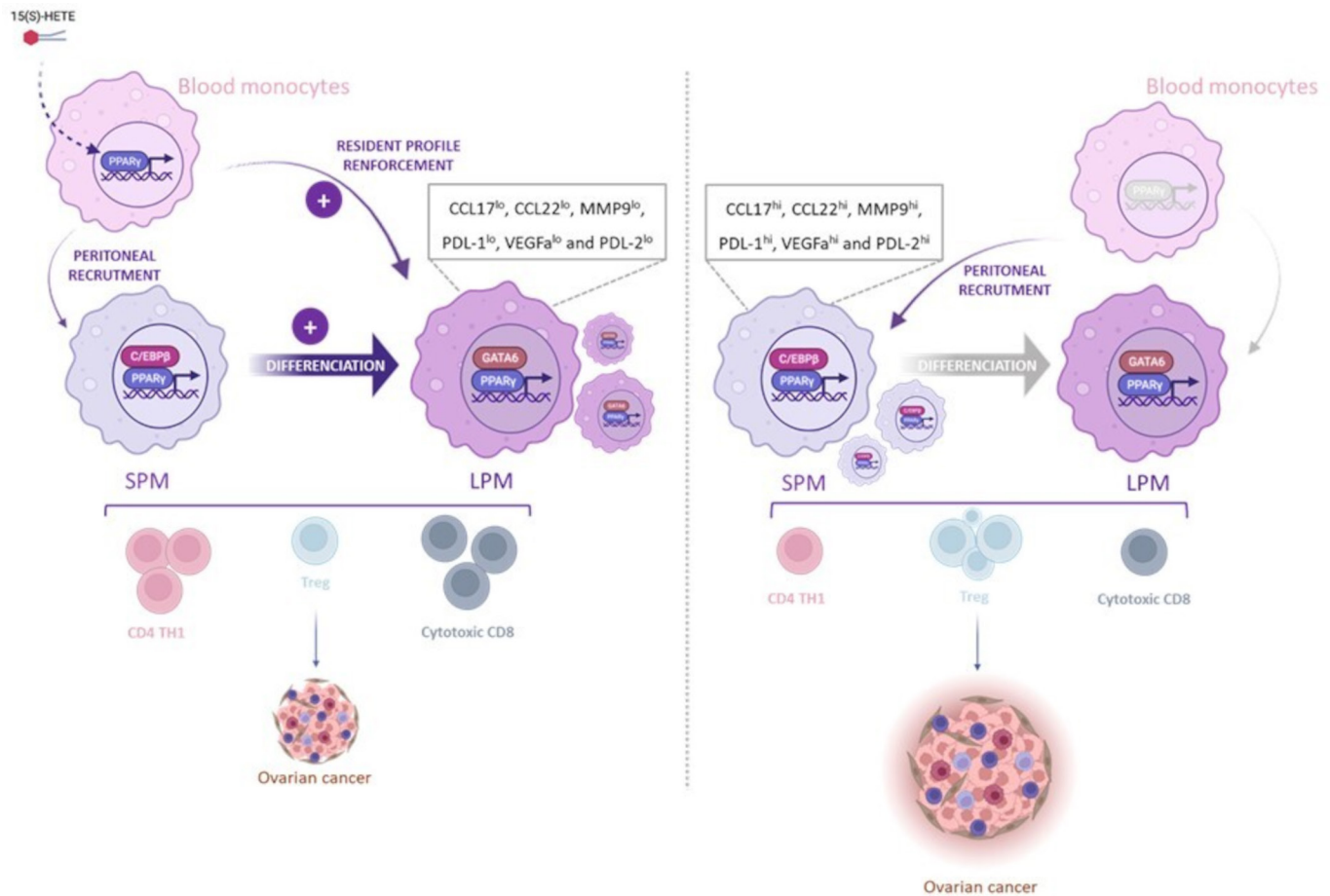


**Figure 8** Schematic illustration of the 15(S)-HETE treatment on ovarian peritoneal carcinomatosis. In a murine experimental model of ovarian peritoneal carcinomatosis, the treatment with 15(S)-HETE, an endogenous PPAR $\gamma$  ligand, induces a significant inhibition of tumor development. The 15(S)-HETE antitumor activity is mediated through PPAR $\gamma$  of macrophages. 15(S)-HETE treatment also orients the peritoneal macrophage population balance towards immunocompetent LPM at the expense of immunosuppressive SPM by promoting SPM-to-LPM differentiation and LPM peritoneal residence. As a result, cytotoxic CD8 $^{+}$  and Th1 CD4 $^{+}$  are strongly recruited and Tregs recruitment is decreased in the ascites of 15(S)-HETE treated tumor-bearing mice. C/EBP $\beta$ , CCAAT/enhancer binding protein  $\beta$ ; CCL-, C-C motif chemokine ligand-; HETE, hydroxyicosatetraenoic acid; LPM, large peritoneal macrophages; MMP9, matrix metalloproteinase; mRNA, PDL-, programmed death-ligand-; PPAR $\gamma$ , peroxisome proliferator-activated receptor  $\gamma$ ; SPM, small peritoneal macrophages; Th1, T helper 1; Treg, regulatory T cell; VEGFa: vascular endothelial growth factor.

of tumor bearing mice. Overall, as compared with SPM, LPM highly expressed mRNA levels of *Ccl3*, *Ccl4*, *Cxcl9* (CXC chemokine ligand 9) and *Cxcl10* (figure 4A, online supplemental table 3). Although *Ccl17* and *Ccl22* encoding immunosuppressive chemokines were highly expressed in SPM, they were almost undetectable in LPM. Consistently, LPM weakly expressed immunosuppressive markers *Cd274* (PDL-1), *Pdcd1lg2* (PDL-2), *Ido2* (indoleamine 2,3-dioxygenase 2), *Tgfb* (tumor growth factor- $\beta$ ) and *Il10* (figure 4A). *Mmp9* (matrix metalloproteinase 9) and *Vegfa* (vascular endothelial growth factor- $\alpha$ ) were also lowly expressed in LPM (figure 4A, online supplemental table 3). *Tnfa* (tumor necrosis factor- $\alpha$ ) was expressed similarly in SPM and LPM (figure 4A, online supplemental table 3). Although the 15(S)-HETE treatment did not affect the expression of *Ccl3*, *Ccl4*, *Cxcl9*, *Cxcl10*, *Ccl17*, *Cd274*, *Mmp9*, *Vegfa* and *Tgfb* in either SPM or LPM, it significantly decreased the expression of *Ccl22*,

*Pdcd1lg2*, *Ido2* and *Il10* in SPM (figure 4A, online supplemental table 3).

Consistent with LPM accumulation and decreased tolerance signature in LPM following 15(S)-HETE treatment, protein levels of CCL3, CCL4, CXCL9, CXCL10 were increased whereas those of CCL22 and CCL17 were decreased in ascites of 15(S)-HETE-treated tumor bearing mice from day 18 post-ID8 injection (figure 4B). In line with decreased immunosuppressive markers, the IL-10 protein level was strongly reduced in ascites from 15(S)-HETE-treated tumor bearing mice (figure 4B). Conversely, protein levels of IL-1 $\beta$  and TNF- $\alpha$  were increased in ascites from 15(S)-HETE-treated tumor bearing mice (figure 4B).

Altogether, these data demonstrate that the antitumor effect of 15(S)-HETE treatment is mediated by the increase of immunocompetent LPM frequency in ascites, which contributes to counteract cancer immunosuppression.

### 15(S)-HETE treatment improves the effector/regulatory T-cell ratio in tumor ascites through a macrophage-dependent mechanism

To investigate whether the 15(S)-HETE treatment-induced SPM/LPM balance change increased immune cell recruitment and activation in the tumor microenvironment, we first evaluated immune populations in ascites. Although the infiltration of natural killer cells (NK1.1+ cells) and macrophages (F4/80+ cells) did not change during tumor progression, CD4 (CD3+ CD4+ CD25-) and CD8 (CD3+ CD8+) T cells, Tregs (CD4+ CD25+ FOXP3+) and B cells (CD19+) were significantly increased (figure 5A). Although the 15(S)-HETE treatment did not alter numbers of macrophages and B cells in ascites, it significantly increased numbers of CD4 and CD8 T cells at day 35 and significantly decrease the number of FoxP3+ Tregs from day 18 after tumor cell injection (figure 5A).

Because the tumor microenvironment is generally considered to be immunosuppressive, we then evaluated whether the 15(S)-HETE treatment promoted the activation of CD4 and CD8 T cells. The 15(S)-HETE treatment contributed to polarizing CD4 T cells toward the Th1 subset (figure 5B). Moreover, the proportion of CD183+ CD8 T cells, a subset with enhanced cytotoxic potential, was significantly increased in ascites from 15(S)-HETE-treated tumor bearing mice (figure 5C). Consistent with these findings, T cells (CD3+) isolated from ascites of 15(S)-HETE-treated tumor-bearing mice expressed higher mRNA levels of perforin (*Prf1*), granzyme B (*Gzmb*) and Fas-ligand (*Faslg*) (figure 5D). Thus, 15(S)-HETE treatment promoted the recruitment of effective Th1 and cytotoxic T lymphocytes and decreased Tregs frequency in tumor ascites. The 15(S)-HETE treatment of tumor-bearing mice deficient of the recombination-activating gene *Rag2* did not decrease the tumor burden of peritoneal membrane, diaphragm or ascites (figure 5E), further supporting the importance of lymphocytes in the antitumor activity of 15(S)-HETE.

We then investigated whether the impact of 15(S)-HETE on T cells was mediated through macrophages. The decrease of Tregs frequency and increases of effective Th1 CD4 cells and cytotoxic CD8 T cells in tumor ascites of 15(S)-HETE-treated tumor-bearing mice were totally abrogated after clodronate treatment (figure 5F–H), supporting that 15(S)-HETE treatment promoted a T cell-dependent antitumor response through macrophages.

### The antitumor activity of 15(S)-HETE is mediated by PPAR $\gamma$ in macrophages

To further dissect how 15(S)-HETE mediated its antitumor effect, we assessed the tumor burden in tumor-bearing mice in which the PPAR $\gamma$  gene was selectively disrupted in myeloid-derived cells (PPAR $\gamma^{M-/-}$ ). Tumor burdens in PPAR $\gamma^{M-/-}$  mice were higher than those in wild-type mice (figure 6A). Consistently, LPM were almost absent in ascites from PPAR $\gamma^{M-/-}$  (figure 6B). Moreover, CD4 and CD8 T-cell infiltrations were lower while the infiltration of Tregs was significantly higher in PPAR $\gamma^{M-/-}$  mice than

in PPAR $\gamma^{M+/+}$  mice (figure 6C). These data suggested an antitumor role of PPAR $\gamma$  in macrophages during OVAD development.

Unlike in PPAR $\gamma^{M+/+}$  mice, 15(S)-HETE treatment did not decrease the SPM frequency and did not increase the LPM frequency and the number of CD4 or CD8 T cells, and did not decrease the number of FOXP3+ Tregs in ascites in tumor-bearing PPAR $\gamma^{M-/-}$  mice (figure 6B–C). The 15(S)-HETE treatment also did not increase frequencies of Th1 CD4 T cells and cytotoxic CD183+ CD8 T cells in tumor-bearing PPAR $\gamma^{M-/-}$  mice (figure 6D–E).

The role of PPAR $\gamma$  in the antitumor activity of 15(S)-HETE was further supported by decreased tumor burden, restored LPM/SPM ratio and increased expression of C/EBP $\beta$  and GATA6 genes and their target genes in tumor-bearing mice treated with rosiglitazone, a synthetic PPAR $\gamma$ -specific agonist<sup>55</sup> (online supplemental S3).

Altogether these results indicate that PPAR $\gamma$  acts in the signaling cascade leading to the inhibition of tumor development, the LPM accumulation in ascites and the enhancement of the effector T cells/Tregs ratio following 15(S)-HETE treatment.

### 15(S)-HETE promotes the differentiation and the peritoneal attachment and attenuates immunosuppressive properties of human ovarian TAMs

Three macrophage subsets (infiltrated, intermediate and resident macrophages) with distinct phenotypes and functions have been described in women's peritoneal cavity.<sup>56</sup> To validate above findings from the murine model in patients, we first evaluated macrophage proportions in cells isolated from the ascites of patients with ovarian cancer. We found that infiltrated macrophages (CD14<sup>inter</sup> CD16<sup>low</sup>) were most abundant whereas there were very few intermediate macrophages (CD14<sup>inter</sup> CD16<sup>inter</sup>) and no resident macrophages (CD14<sup>high</sup> CD16<sup>high</sup>) (figure 7A,B).

Consistent with findings in mice, 15(S)-HETE treatment induced expressions of *ITGAM* (CD11b) and *ALOX15*, slightly reduced *HLADR* expression, and did not significantly affect *CLECTA* (Dectin-1) expression (figure 7C). The 15(S)-HETE treatment also enhanced the expression of C/EBP $\beta$  and GATA6 genes and their target genes (*CYP27B1*, *LGALS3*, *SELP*, *SERPINB2*, *THBS1*), suggesting that 15(S)-HETE treatment could activate the differentiation of macrophages isolated from human ovarian cancer ascites towards LPM-like macrophages and could favor their maintenance in the peritoneal cavity (figure 7D). Moreover, 15(S)-HETE treatment decreased mRNA levels of *CD274*, *PDCD1LG2*, *CCL17*, *CCL22*, and *MMP9* (figure 7E). These data indicated that 15(S)-HETE had similar effects on human TAMs as on mouse TAMs.

### DISCUSSION

The growth of ovarian cancer is associated with the development of peritoneal ascites containing proinflammatory soluble factors and cellular components that provide a tumor-promoting microenvironment.<sup>6</sup>

Here, we report that 15(S)-HETE treatment inhibits tumor progression in a mouse model of OVAD that is mediated through PPAR $\gamma$  in macrophages. Consistently, PPAR $\gamma^{+/-}$  mice have an increased susceptibility toward 7,12-dimethylbenz[a]anthracene (DMBA)-mediated breast, skin and ovarian carcinogenesis.<sup>41</sup>

We showed that the SPM frequency strongly increases while the percentage of LPM decreases in the peritoneal cavity of untreated tumor-bearing mice. Consistently, SPM mobilization in response to IL-17 in the same murine model of ovarian cancer is associated with tumor progression.<sup>28</sup> Interestingly, we demonstrate that the 15(S)-HETE treatment modulates the SPM/LPM balance in ascites to closer to that in mice without tumor. In agreement with the ability of SPM to promote ovarian cancer development,<sup>28</sup> our study characterizes SPM as immunosuppressive, which is supported by reports showing that only monocyte-derived alternative activated macrophages express PDL-2 and can induce FoxP3<sup>+</sup> Tregs differentiation.<sup>57,58</sup> Thus, the effect of 15(S)-HETE treatment on the increase of LPM frequency in ascites could counteract SPM-mediated immunosuppression. Consistently, 15(S)-HETE treatment promotes the infiltration of CD4<sup>+</sup> Th1 T cells and cytotoxic CD8<sup>+</sup> T cells in ascites. We also establish that the weak expression of CCL17 and CCL22 in LPM of 15(S)-HETE-treated mice is correlated with a strong decrease in the Tregs number in ascites. These data support that 15(S)-HETE enhances the effector T cells/Tregs ratio through the orientation of immunoregulatory SPM toward LPM, which contribute to attract and activate effector immune cells. These observations highlight the involvement of macrophages in T cell-dependent antitumor response on 15(S)-HETE treatment.

This study also reveals that the SPM-to-LPM differentiation induced by the 15(S)-HETE treatment involves PPAR $\gamma$  and C/EBP $\beta$ , which is supported by reported close functional and physical links between C/EBP $\beta$  and PPAR $\gamma$ <sup>29</sup> and crucial role of C/EBP $\beta$  in SPM-to-LPM differentiation.<sup>27</sup> Furthermore, our results indicate that 15(S)-HETE treatment contributes to the maintenance of LPM in the peritoneal cavity by increasing the expression of GATA6, known to be involved in LPM residency in the peritoneum,<sup>26</sup> and adhesion proteins, such as Thbs1, CD62p and Serpinb2, encoded by GATA6-target genes.<sup>59</sup> These results are also consistent with the PPAR $\gamma$  activation in the preservation of GATA6 expression in bone-marrow derived mast cells<sup>31</sup> and with the inhibitory effect of 15(S)-HETE treatment on neutrophil migration in inflammatory conditions.<sup>60</sup> Resident macrophage migration to the omentum has been associated with the spread of ovarian cancer cells to the same site, which worsens the prognosis.<sup>61</sup> These data strengthen the importance of maintaining LPM in the peritoneal cavity. To further validate the requirement of C/EBP $\beta$  and GATA6 on PPAR $\gamma$  activation for SPM-to-LPM differentiation, it would be interesting to evaluate LPM differentiation and migration by genetically invalidating C/EBP $\beta$  and GATA6.

Finally, we demonstrate PPAR $\gamma$  as a key component in the 15(S)-HETE-triggered signaling cascade that promotes T-cell antitumor response. Although several studies have shown that PPAR $\gamma$  induces TAM polarization toward M2 protumor phenotype via their ability to suppress T-cell response,<sup>62,63</sup> other findings showed that in T-cell lymphoma and OVAD PPAR $\gamma$  activation was able to induce an antitumor phenotype of macrophages through the conversion of tumor supporting macrophages to cytotoxic effectors.<sup>34</sup> Several studies have also indicated that PPAR $\gamma$  has immunostimulatory activities.<sup>17,64,65</sup> Indeed, mice deficient of PPAR $\gamma$  selectively in myeloid cells have a decreased CD8<sup>+</sup> T effectors to Tregs ratio and an impaired tumor rejection with granulocyte-macrophage colony-stimulating factor (GM-CSF)-secreting tumor-cell vaccines.<sup>64</sup> Moreover, PPAR $\gamma$  ligands reverse cytotoxic T lymphocyte suppression induced by TAMs and decrease Tregs infiltration.<sup>17,65</sup> PPAR $\gamma$  activation has already been suggested to directly suppress tumor cells.<sup>38</sup> Indeed, PPAR $\gamma$  and its ligands are documented to induce differentiation, growth inhibition and apoptosis of cell lines derived from several types of cancer, including human ovarian cancer, in vitro and in vivo.<sup>66-70</sup> PPAR $\gamma$  ligands have also been shown to potently inhibit angiogenesis.<sup>71</sup> Synergistic therapeutic effects have been also observed between PPAR $\gamma$  ligands and conventional chemotherapy drugs.<sup>38,72,73</sup> Despite studies indicating a conflicting role for PPAR $\gamma$  activation in macrophage differentiation during tumor development, most studies strengthen the use of PPAR $\gamma$  agonists in anticancer therapy.

The use of 15(S)-HETE as an antitumor agent is also supported by the robust downregulation of 15-LOX in various human cancers<sup>74,75</sup> and by the significant decrease of the 15-HETE concentration in advanced epithelial ovarian cancer ascites.<sup>35</sup> Many lines of evidence suggest that 5-LOX and 12-LOX metabolites promote angiogenesis, carcinogenesis and tumor cell proliferation.<sup>76-78</sup> Agents that shift the balance of LOX activities from procarcinogenic (12-HETE and 5-HETE) to anticarcinogenic (15(S)-HETE) metabolism of polyunsaturated fatty acids therefore have been proposed as approaches for cancer prevention and/or treatment.

In conclusion, we show that 15(S)-HETE has an antitumor activity in a murine model of OVAD that is mediated through promoting the differentiation of SPM to LPM and maintaining LPM in the peritoneum. LPM contribute to counteract cancer immunosuppression and to attract effector immune T cells (figure 8). These results also establish a critical role of PPAR $\gamma$  in macrophages in the 15(S)-HETE-triggered inhibition of OVAD development, strengthening the use of PPAR $\gamma$  agonists in anticancer therapy.

#### Author affiliations

<sup>1</sup>RESTORE Research Center, Université de Toulouse, INSERM-1301, CNRS-5070, EFS, ENV, Toulouse, France

<sup>2</sup>UMR1037 Centre de Recherche en Cancérologie de Toulouse (CRCT), Université de Toulouse, INSERM, Toulouse, France

<sup>3</sup>Institut Claudius Regaud, IUCT Oncopole, Toulouse, France

**Acknowledgements** We thank Philippe Batigne (Université Paul Sabatier) and Dimitri Marsal (INSERM) for excellent technical support, Alexia Zakaroff-Girard, Elodie Riant and Jessica Fontaine (TRI imaging platform, IFR150/I2MC/Restore) for flow cytometry technical assistance. This manuscript was edited at Life Science Editors.

**Contributors** MR has been added to the list of coauthors, as she carried out the cytometry experiments for the review. M-LR has changed position for her participation in the cytometry experiments for the revision. CB is now co-first and LL is now co-last author as they designed, carried out and analyzed the experiments for the revision of the paper. AC is responsible for the overall content as guarantor.

**Funding** This work was funded by a grant from the French government (Idex 2012) and the Groupe de recherche de l'Institut Claudius Regaud (GRICR).

**Competing interests** None declared.

**Patient consent for publication** Consent obtained directly from patient(s).

**Ethics approval** This study involves human participants and was approved by Comités de protection des personnes (CPP) ARS Approval ID number: 2019-A00195-52. Participants gave informed consent to participate in the study before taking part.

**Provenance and peer review** Not commissioned; externally peer reviewed.

**Data availability statement** All data relevant to the study are included in the article or uploaded as supplementary information.

**Supplemental material** This content has been supplied by the author(s). It has not been vetted by BMJ Publishing Group Limited (BMJ) and may not have been peer-reviewed. Any opinions or recommendations discussed are solely those of the author(s) and are not endorsed by BMJ. BMJ disclaims all liability and responsibility arising from any reliance placed on the content. Where the content includes any translated material, BMJ does not warrant the accuracy and reliability of the translations (including but not limited to local regulations, clinical guidelines, terminology, drug names and drug dosages), and is not responsible for any error and/or omissions arising from translation and adaptation or otherwise.

**Open access** This is an open access article distributed in accordance with the Creative Commons Attribution Non Commercial (CC BY-NC 4.0) license, which permits others to distribute, remix, adapt, build upon this work non-commercially, and license their derivative works on different terms, provided the original work is properly cited, appropriate credit is given, any changes made indicated, and the use is non-commercial. See <http://creativecommons.org/licenses/by-nc/4.0/>.

#### ORCID iD

Agnès Coste <http://orcid.org/0000-0001-7781-3323>

#### REFERENCES

- Khazaei Z, Seyedeh Mahdih N, Reza B, *et al.* Worldwide incidence and mortality of ovarian cancer and human development index (HDI): GLOBOCAN sources and methods 2018. *J Prev Med Hyg* 2021;62:E174–84.
- Sopik V, Iqbal J, Rosen B, *et al.* Why have ovarian cancer mortality rates declined? part I. *Gynecologic Oncology* 2015;138:741–9.
- Sainz de la Cuesta R, Eichhorn JH, Rice LW, *et al.* Histologic transformation of benign Endometriosis to early epithelial ovarian cancer. *Gynecologic Oncology* 1996;60:238–44.
- Ness RB, Grisso JA, Cottreau C, *et al.* Factors related to inflammation of the ovarian epithelium and risk of ovarian cancer. *Epidemiology* 2000;11:111–7.
- Risch HA, Howe GR. Pelvic inflammatory disease and the risk of epithelial ovarian cancer. *Cancer Epidemiol Biomarkers Prev* 1995;4:447–51.
- Ahmed N, Stenvers KL. Getting to know ovarian cancer ascites: opportunities for targeted therapy-based translational research. *Front Oncol* 2013;3:256.
- Le Naour A, Prat M, Thibault B, *et al.* Tumor cells educate mesenchymal stromal cells to release chemoprotective and immunomodulatory factors. *J Mol Cell Biol* 2020;12:202–15.
- Wang X, Deavers M, Patenia R, *et al.* Monocyte/macrophage and T-cell infiltrates in peritoneum of patients with ovarian cancer or benign pelvic disease. *J Transl Med* 2006;4:30.
- Chanmee T, Ontong P, Konno K, *et al.* Tumor-associated macrophages as major players in the tumor microenvironment. *Cancers (Basel)* 2014;6:1670–90.
- Lewis CE, Pollard JW. Distinct role of macrophages in different tumor microenvironments. *Cancer Res* 2006;66:605–12.
- Elgert KD, Alleva DG, Mullins DW. Tumor-induced immune dysfunction: the macrophage connection. *J Leukoc Biol* 1998;64:275–90.
- Sharma P, Allison JP. The future of immune checkpoint therapy. *Science* 2015;348:56–61.
- Noy R, Pollard JW. Tumor-associated macrophages: from mechanisms to therapy. *Immunity* 2014;41:49–61.
- Biswas SK, Sica A, Lewis CE. Plasticity of macrophage function during tumor progression: regulation by distinct molecular mechanisms. *J Immunol* 2008;180:2011–7.
- Cho U, Kim B, Kim S, *et al.* Pro-inflammatory M1 macrophage enhances metastatic potential of ovarian cancer cells through NF-KB activation. *Mol Carcinog* 2018;57:235–42.
- Robinson-Smith TM, Isaacsohn I, Mercer CA, *et al.* Macrophages mediate inflammation-enhanced metastasis of ovarian tumors in mice. *Cancer Res* 2007;67:5708–16.
- Van Ginderachter JA, Meerschaet S, Liu Y, *et al.* Peroxisome proliferator-activated receptor  $\gamma$  (PPAR $\gamma$ ) ligands reverse CTL suppression by alternatively activated (M2) macrophages in cancer. *Blood* 2006;108:525–35.
- Kiss M, Van Gassen S, Movahedi K, *et al.* Myeloid cell heterogeneity in cancer: not a single cell alike. *Cell Immunol* 2018;330:188–201.
- Van Overmeire E, Laoui D, Keirsse J, *et al.* Mechanisms driving macrophage diversity and specialization in distinct tumor microenvironments and parallels with other tissues. *Front Immunol* 2014;5:127.
- Ginhoux F, Greter M, Leboeuf M, *et al.* Fate mapping analysis reveals that adult Microglia derive from primitive Macrophages. *Science* 2010;330:841–5.
- Hashimoto D, Chow A, Noizat C, *et al.* Tissue-resident macrophages self-maintain locally throughout adult life with minimal contribution from circulating monocytes. *Immunity* 2013;38:792–804.
- Yona S, Kim K-W, Wolf Y, *et al.* Fate mapping reveals origins and dynamics of monocytes and tissue macrophages under homeostasis. *Immunity* 2013;38:79–91.
- Ghosh EEB, Cassado AA, Govoni GR, *et al.* Two physically, functionally, and developmentally distinct peritoneal macrophage subsets. *Proc Natl Acad Sci U S A* 2010;107:2568–73.
- Cassado ADA, D'Império Lima MR, Bortoluci KR. Revisiting Mouse peritoneal Macrophages: heterogeneity, development, and function. *Front Immunol* 2015;6:225.
- Barth MW, Hendrzak JA, Melnicoff MJ, *et al.* Review of the macrophage disappearance reaction. *J Leukoc Biol* 1995;57:361–7.
- Okabe Y, Medzhitov R. Tissue-specific signals control reversible program of localization and functional polarization of macrophages. *Cell* 2014;157:832–44.
- Cain DW, O'Koren EG, Kan MJ, *et al.* Identification of a tissue-specific, C/EBP $\beta$ -dependent pathway of differentiation for murine peritoneal Macrophages. *J Immunol* 2013;191:4665–75.
- Rei M, Gonçalves-Sousa N, Lança T, *et al.* Murine Cd27(–) V $\gamma$ 6(+)  $\Gamma\delta$  T cells producing IL-17A promote ovarian cancer growth via mobilization of Protumor small peritoneal Macrophages. *Proc Natl Acad Sci U S A* 2014;111:E3562–70.
- Farmer SR. Regulation of Ppargamma activity during Adipogenesis. *Int J Obes (Lond)* 2005;29 Suppl 1:S13–6.
- Madsen MS, Siersbæk R, Boergesen M, *et al.* Peroxisome Proliferator-activated receptor  $\Gamma$  and C/EBP $\alpha$  synergistically activate key metabolic Adipocyte genes by assisted loading. *Mol Cell Biol* 2014;34:939–54.
- Tachibana M, Wada K, Katayama K, *et al.* Activation of peroxisome Proliferator-activated receptor gamma suppresses mast cell maturation involved in allergic diseases. *Allergy* 2008;63:1136–47.
- Marion-Letellier R, Savoye G, Ghosh S. Fatty acids, Eicosanoids and PPAR gamma. *Eur J Pharmacol* 2016;785:44–9.
- Lefèvre L, Authier H, Stein S, *et al.* LRH-1 mediates anti-inflammatory and antifungal phenotype of IL-13-activated Macrophages through the PPAR $\gamma$  ligand synthesis. *Nat Commun* 2015;6:6801.
- Alaeddine M, Prat M, Poinso V, *et al.* IL13-mediated Dectin-1 and mannose receptor overexpression promotes macrophage antitumor activities through recognition of sialylated tumor cells. *Cancer Immunol Res* 2019;7:321–34.
- Freedman RS, Wang E, Voiculescu S, *et al.* Comparative analysis of peritoneum and tumor eicosanoids and pathways in advanced ovarian cancer. *Clin Cancer Res* 2007;13:5736–44.



- 36 Hennig R, Kehl T, Noor S, *et al.* 15-Lipoxygenase-1 production is lost in Pancreatic cancer and overexpression of the gene inhibits tumor cell growth. *Neoplasia* 2007;9:917–26.
- 37 Shappell SB, Boeglin WE, Olson SJ, *et al.* 15-Lipoxygenase-2 (15-LOX-2) is expressed in benign Prostatic epithelium and reduced in prostate adenocarcinoma. *Am J Pathol* 1999;155:235–45.
- 38 Robbins GT, Nie D. PPAR gamma, bioactive lipids, and cancer progression. *Front Biosci (Landmark Ed)* 2012;17:1816–34.
- 39 Suh N, Wang Y, Williams CR, *et al.* A new ligand for the peroxisome proliferator-activated receptor- $\Gamma$  (PPAR- $\Gamma$ ), Gw7845, inhibits rat mammary carcinogenesis. *Cancer Res* 1999;59:5671–3.
- 40 Yin Y, Russell RG, Dettin LE, *et al.* Peroxisome proliferator-activated receptor  $\Delta$  and  $\Gamma$  agonists differentially alter tumor differentiation and progression during mammary carcinogenesis. *Cancer Res* 2005;65:3950–7.
- 41 Nicol CJ, Yoon M, Ward JM, *et al.* Ppargamma influences susceptibility to DMBA-induced Mammary, ovarian and skin carcinogenesis. *Carcinogenesis* 2004;25:1747–55.
- 42 Niu S, Cui B, Huang J, *et al.* PPAR $\gamma$  is correlated with prognosis of epithelial ovarian cancer patients and affects tumor cell progression in vitro. 2017. Available: <https://www.semanticscholar.org/paper/PPAR%CE%B3-is-correlated-with-prognosis-of-epithelial-in-Niu-Cui/1ef90c884388dab19b083b16290beb90ea2176f8>
- 43 Hatton JL, Yee LD. Clinical use of Ppargamma ligands in cancer. *PPAR Res* 2008;2008:159415.
- 44 Reddy AT, Lakshmi SP, Reddy RC. PPAR $\gamma$  as a novel therapeutic target in lung cancer. *PPAR Res* 2016;8972570.
- 45 Ryu S, Kim DS, Lee MW, *et al.* Anti-Leukemic effects of PPAR $\gamma$  ligands. *Cancer Lett* 2018;418:10–9.
- 46 Reichle A, Bross K, Vogt T, *et al.* Pioglitazone and rofecoxib combined with angiostatically scheduled trofosfamide in the treatment of far-advanced melanoma and soft tissue sarcoma. *Cancer* 2004;101:2247–56.
- 47 Mueller E, Smith M, Sarraf P, *et al.* Effects of ligand activation of peroxisome proliferator-activated receptor  $\Gamma$  in human prostate cancer. *Proc Natl Acad Sci U S A* 2000;97:10990–5.
- 48 Roby KF, Taylor CC, Sweetwood JP, *et al.* Development of a syngeneic mouse model for events related to ovarian cancer. *Carcinogenesis* 2000;21:585–91.
- 49 Couderc B, Pradines A, Rafii A, *et al.* In vivo restoration of Rhob expression leads to ovarian tumor regression. *Cancer Gene Ther* 2008;15:456–64.
- 50 Galès A, Conduché A, Bernad J, *et al.* PPAR $\gamma$  controls dectin-1 expression required for host antifungal defense against *Candida albicans*. *PLoS Pathog* 2010;6:e1000714.
- 51 Lefèvre L, Lugo-Villarino G, Meunier E, *et al.* The C-type lectin receptors Dectin-1, MR, and Signr3 contribute both positively and negatively to the macrophage response to *Leishmania Infantum*. *Immunity* 2013;38:1038.
- 52 van Vloten JP, Matuszewska K, Minow MAA, *et al.* Oncolytic Orf virus licenses NK cells via Cdc1 to activate innate and adaptive antitumor mechanisms and extends survival in a murine model of late-stage ovarian cancer. *J Immunother Cancer* 2022;10:e004335.
- 53 Sastourné-Arrey Q, Mathieu M, Contreras X, *et al.* Adipose tissue is a source of regenerative cells that augment the repair of skeletal muscle after injury. *Nat Commun* 2023;14:80.
- 54 Hamburger AW, Dunn FE, White CP. Percoll density gradient separation of cells from human malignant effusions. *Br J Cancer* 1985;51:253–8.
- 55 Lehmann JM, Moore LB, Smith-Oliver TA, *et al.* An antidiabetic Thiazolidinedione is a high affinity ligand for peroxisome proliferator-activated receptor  $\Gamma$  (PPAR $\gamma$ ) \*. *J Biol Chem* 1995;270:12953–6.
- 56 Ruiz-Alcaraz AJ, Carmona-Martínez V, Tristán-Manzano M, *et al.* Characterization of human peritoneal monocyte/macrophage Subsets in homeostasis: phenotype, Gata6, Phagocytic/oxidative activities and Cytokines expression. *Sci Rep* 2018;8:12794.
- 57 Bowman RL, Klemm F, Akkari L, *et al.* Macrophage Ontogeny underlies differences in tumor-specific education in brain malignancies. *Cell Rep* 2016;17:2445–59.
- 58 Gundra UM, Girgis NM, Ruckerl D, *et al.* Alternatively activated Macrophages derived from monocytes and tissue macrophages are Phenotypically and functionally distinct. *Blood* 2014;123:e110–22.
- 59 Schroder WA, Hirata TD, Le TT, *et al.* Serpinb2 inhibits migration and promotes a resolution phase signature in large peritoneal macrophages. *Sci Rep* 2019;9:12421.
- 60 Takata S, Papayianni A, Matsubara M, *et al.* 15-Hydroxyeicosatetraenoic acid inhibits neutrophil migration across cytokine-activated endothelium. *Am J Pathol* 1994;145:541–9.
- 61 Etzerodt A, Moulin M, Doktor TK, *et al.* Tissue-resident Macrophages in Omentum promote metastatic spread of ovarian cancer. *J Exp Med* 2020;217:e20191869.
- 62 Deng X, Zhang P, Liang T, *et al.* Ovarian cancer stem cells induce the M2 polarization of Macrophages through the PPAR $\gamma$  and NF-KB pathways. *Int J Mol Med* 2015;36:449–54.
- 63 Liu S, Zhang H, Li Y, *et al.* S100A4 enhances Protumor macrophage polarization by control of PPAR- $\Gamma$ -dependent induction of fatty acid oxidation. *J Immunother Cancer* 2021;9:e002548.
- 64 Goyal G, Wong K, Nirschl CJ, *et al.* PPAR $\gamma$  contributes to immunity induced by cancer cell vaccines that Secrete GM-CSF. *Cancer Immunol Res* 2018;6:723–32.
- 65 Gutting T, Weber CA, Weidner P, *et al.* PPAR $\gamma$ -activation increases intestinal M1 Macrophages and mitigates formation of Serrated adenomas in mutant KRAS mice. *Oncimmunology* 2018;7:e1423168.
- 66 Elstner E, Müller C, Koshizuka K, *et al.* Ligands for peroxisome Proliferator-activated Receptorgamma and retinoic acid receptor inhibit growth and induce apoptosis of human breast cancer cells in vitro and in BNX mice. *Proc Natl Acad Sci U S A* 1998;95:8806–11.
- 67 de Jong E, Winkel P, Poelstra K, *et al.* Anticancer effects of 15D-prostaglandin-J2 in wild-type and doxorubicin-resistant ovarian cancer cells: novel actions on Sirt1 and HDAC. *PLoS One* 2011;6:e25192.
- 68 Kim S, Lee J-J, Heo DS. PPAR $\gamma$  ligands induce growth inhibition and apoptosis through P63 and P73 in human ovarian cancer cells. *Biochemical and Biophysical Research Communications* 2011;406:389–95.
- 69 Kubota T, Koshizuka K, Williamson EA, *et al.* Ligand for peroxisome Proliferator-activated receptor  $\Gamma$  (Troglitazone) has potent antitumor effect against human prostate cancer both in vitro and in vivo. *Cancer Res* 1998;58:3344–52.
- 70 Tontonoz P, Singer S, Forman BM, *et al.* Terminal differentiation of human Liposarcoma cells induced by ligands for peroxisome Proliferator-activated receptor gamma and the Retinoid X receptor. *Proc Natl Acad Sci U S A* 1997;94:237–41.
- 71 Giaginis C, Tsantili-Kakoulidou A, Theocharis S. Peroxisome Proliferator-activated receptor-gamma ligands: potential pharmacological agents for targeting the angiogenesis signaling Cascade in cancer. *PPAR Res* 2008;2008:431763.
- 72 Girnun GD, Chen L, Silvaggi J, *et al.* Regression of drug-resistant lung cancer by the combination of rosiglitazone and carboplatin. *Clin Cancer Res* 2008;14:6478–86.
- 73 Girnun GD, Naseri E, Vafai SB, *et al.* Synergy between Ppargamma ligands and platinum-based drugs in cancer. *Cancer Cell* 2007;11:395–406.
- 74 Subbarayan V, Xu X-C, Kim J, *et al.* Inverse relationship between 15-Lipoxygenase-2 and PPAR-gamma gene expression in normal epithelia compared with tumor epithelia. *Neoplasia* 2005;7:280–93.
- 75 Tian R, Zuo X, Jaoude J, *et al.* Alox15 as a suppressor of inflammation and cancer: lost in the link. *Prostaglandins Other Lipid Mediat* 2017;132:77–83.
- 76 Guo AM, Liu X, Al-Wahab Z, *et al.* Role of 12-Lipoxygenase in regulation of ovarian cancer cell proliferation and survival. *Cancer Chemother Pharmacol* 2011;68:1273–83.
- 77 Moreno JJ. New aspects of the role of Hydroxyeicosatetraenoic acids in cell growth and cancer development. *Biochem Pharmacol* 2009;77:1–10.
- 78 Pidgeon GP, Lysaght J, Krishnamoorthy S, *et al.* Lipoxygenase metabolism: roles in tumor progression and survival. *Cancer Metastasis Rev* 2007;26:503–24.